Title
HIGH TEMPERATURE PHASE EQUILIBRIA IN THE LEAD TITANTE-LEAD ZIRCONATE SYSTEM

Author
Moon, Ronald L.

Publication Date
1967-05-01

UCRL-17545

University of California

Ernest O. Lawrence Radiation Laboratory

HIGH TEMPERATURE PHASE EQUILIBRIA IN THE LEAD TITANATE-LEAD ZIRCONATE SYSTEM

Ronald L. Moon

(Ph. D. Thesis)

May 1967

Berkeley, California

DISCLAIMER

UCRL-17545

UNIVERSITY OF CALIFORNIA

Lawrence Radiation Laboratory
Berkeley, California

AEC Contract W-7405-eng-48

HIGH TEMPERATURE PHASE EQUILIBRIA IN THE LEAD TITANATE-LEAD ZIRCONATE SYSTEM

Ronald L. Moon

(Ph.D. Thesis)

May 1967

TABLE OF CONTENTS

HIGH TEMPERATURE PHASE EQUILIBRIA IN THE LEAD TITANATE-LEAD ZIRCONATE SYSTEM

Ronald L. Moon

Inorganic Materials Research Division, Lawrence Radiation Laboratory, and Department of Mineral Technology, College of Engineering, University of California, Berkeley, California

ABSTRACT

May 1967

Phase relationships at elevated temperatures in the lead titanate-lead zirconate system are investigated by vapor loss, X-ray, thermal and differential thermal analyses.

A solid solution is shown to exist in the region between the Curie and solidus temperatures. Experiments in the solid solution region conducted in vacuum at 1050°C and 1100°C show that vaporization of lead oxide results in the formation of a depletion layer at the sample's surface. The depletion layer is deficient in lead oxide and new phases appear as a consequence of this compositional change.

The lowest temperature at which liquid is formed in this system is the melting point of lead titanate, determined to be 1286°±3°C. Increasing the lead zirconate to lead titanate ratio increases the solidus temperature. The highest temperature, the melting point of lead zirconate, cannot be determined because of rapid crucible attack by the sample above 1500°C. At 1360°C a peritectic reaction occurs for compositions between 15 to approximately 40 mole % $PbZrO_3$. Above the peritectic temperature is a three phase region with liquid, zirconia and lead zirconate titanate solid solution in equilibrium. Compositions richer in $PbZrO_3$ than 40 mole % decompose directly to three phases at

the solidus temperatures.

The existence of the three phase region demonstrates that the lead titanate-lead zirconate system is not a true binary, but a subsection of the PbO-TiO_2-ZrO_2 ternary system.

I. INTRODUCTION

Lead zirconate-titanate is currently the primary crystalline solid used for ceramic piezoelectric transducers. Even though it is so widely used, little is known about the phase relationships existing at high temperatures. Since these solids are formed at temperatures between 1100°-1300°C by sintering or hot-pressing methods, information of this nature is necessary for understanding the mechanisms involved in forming dense polycrystalline bodies. In addition, the data is needed for growing single crystals.

The purpose of this study was (1) to investigate whether any high temperature phases do exist in this system, and (2) to determine the solidus and liquidus temperatures of the proposed binary system.

The electrical characteristic making this substance useful is its ferroelectric behavior. This property is fundamental in obtaining ceramic polycrystalline piezoelectric transducers. A polycrystalline specimen will not act in a piezoelectric manner unless the polarity of the crystals shows a preferred orientation. A ferroelectric crystal can realign its direction of polarity (within crystallographic limitations) when subjected to a d.c. electric field. When a d.c. electric field is applied to a polycrystalline sample with randomly oriented domains (regions with the same direction of polarity), the result is a sample with a net polarity created by the domain reorientation during the poling process. Because a ferroelectric crystal is also piezoelectric, a transducer is produced.

The superiority of lead zirconate titanate (PZT) over other possible materials is due to the relatively high Curie temperature and the

piezoelectric constant possessed by the solid solution which is obtained by mixing lead titanate ($PbTiO_3$) with lead zirconate ($PbZrO_3$).

A. $PbTiO_3$

Lead titanate, $PbTiO_3$, crystallizes in the perovskite structure and is ferroelectric below its Curie temperature of 490°C.[1-3] There appears to be a further phase transition at -100°C which occurs only when the crystal is very slowly cooled.[4] This low temperature phase is non-ferroelectric and possesses a multiple tetragonal cell.

In the paraelectric state above the Curie temperature, the cubic or ideal perovskite structure is maintained. On cooling through the Curie temperature, the lattice undergoes a discontinuous change in the c/a ratio of approximately 2%,[5] and at room temperature has a tetragonal structure with the lattice parameters shown in Table I.[6]

In addition to the lattice distortion and high value of the dielectric constant at the Curie temperature, a great abnormality in the specific heat and specific volume is found.[5] The specific heat anomaly yielded an integrated value of 1150 cal/mole over the temperature interval 340° to 540°C. The linear coefficient of thermal expansion of a polycrystalline sample changes sign at the Curie temperature and expands on further cooling.[7]

Diffraction studies employing X-rays and neutron beams have determined the atomic positions of the ions in the ferroelectric state.[8] Shifts in atomic positions are best represented when the oxygen octahedra are assumed to be undisturbed. The lead and titanium ion shifts are then taken relative to an origin in the center of the octahedron (Fig. 1).

TABLE I Lattice parameters of lead titanate and lead zirconate at room temperature

$PbTiO_3$	Tetragonal lattice parameters
	$a = 3.899\text{Å}$
	$c = 4.1532\text{Å}$
	$c/a = 1.065$
$PbZrO_3$	Orthorhombic lattice parameters
	$a = 5.88\text{Å}$
	$b = 11.76\text{Å}$
	$c = 8.20\text{Å}$
	Relationship between the orthorhombic lattice parameters and the tetragonal structure originally proposed
	$a_{rh} = \sqrt{2}a_t$
	$b_{rh} = 2\sqrt{2}a_t$
	$c_{rh} = 2c_t$

The theoretical density as calculated from lattice parameters is 8.02 ± 0.02 gm/cm^3.[9]

The flux method, which uses a suitable solvent from which crystallization is promoted, has been used to grow single crystals; however, difficulty is encountered because of PbO loss at high temperatures. Crystals with edges of several millimeters have been obtained by using compositions of $2PbO \cdot TiO_2$.[9] Larger crystals (1 cm on edge) have been grown using KF as a flux.[10] Other fluxes such as $Pb(BO_2)_2$,[11] Na_2SiO_3,[12] and $PbO\text{-}PbCl_2$ [13] have also been used successfully.

$PbTiO_3$ begins to decompose to PbO vapor and TiO_2 solid when heated above 800°C.[14]

The melting point of $PbTiO_3$ is reported as 1281 ± 3°C,[9] 1285°C,[15] and 1340°C.[16] The latter value was determined by a strip furnace acknowledged to give uncertain values of temperature.

The binary system $PbO\text{-}TiO_2$ has never been studied in its entirety. Two eutectic temperatures have been reported on both sides of $PbTiO_3$. The temperature in the PbO rich region was 838°C and in the TiO_2 rich region was 1240°C.[15] A second study which determined the liquidus temperatures over a composition range from 0 to 25 mole % TiO_2 gave a eutectic temperature at 818°C and eutectic composition of 7.5 mole % TiO_2.[17] This same report mentioned two peritectic reactions present in the system. One peritectic reaction was suggested to occur due to the decomposition of $2PbO \cdot TiO_2$. Subsequent studies, however, have shown no evidence of this compound.[3,9,18] The most convincing of these investigations[18] examined the PbO rich side of the $PbO\text{-}TiO_2$ diagram by firing mixtures of PbO (orthorhombic) and TiO_2 (rutile) at 800°C. The only phases detected by X-ray analysis were $PbTiO_3$ and orthorhombic and

tetragonal PbO. The conclusion is that a PbO solid solution is formed when the orthorhombic PbO dissolves TiO_2 and transforms to tetragonal PbO, and that no compound exists between $PbTiO_3$ and PbO.

B. $PbZrO_3$

Lead zirconate also has the ideal perovskite structure above its Curie temperature of approximately 230°C;[3,19] but on cooling, the situation is more complex. Recent studies[20,21] have shown two-phase transitions to take place about the Curie temperature. The reported transition temperatures obtained by dielectric and expansion measurements differ slightly and are given in Table II.

The transitions observed in $PbZrO_3$ on cooling give a para-electric state above ~ 228°, a ferroelectric state exhibiting a volume expansion on cooling between 228°C and ~ 212°C, and finally an anti-ferroelectric state below 212°C showing a volume contraction on cooling. The intermediate ferroelectric phase will disappear if the calcium impurity content of ZrO_2 is increased.[21]

Calorimetric measurements yield a heat of transition of 440 cal/mole.[22]

At room temperature, the structure is orthorhombic,[23] although it was first identified as tetragonal.[24] This phase is derived from the cubic perovskite lattice by antiparallel displacement of the Pb ions along one of the original ⟨110⟩ directions, called the a axis.[23] (Fig. 2.) Additional detailed studies revealed that the oxygen atoms are also displaced anti-parallel to each other in the (001) plane.[25] The lattice parameters are given in Table I with a and b axes being oriented along the original cubic ⟨110⟩ direction.[23]

The existence of two peritectic reactions at 910°C and 1570°C has been reported.[26] $PbZrO_3$ appears to be the only intermediate compound between PbO and ZrO_2. For example, heating a 20 mole % PbO-80 mole %

TABLE II. Transition temperatures of $PbZrO_3$ near the Curie temp.

	Lower transition temp.	Higher transition temp.	Measurement method	Ref.
Heating	226°C	236°C	Expansion	21
	227°C	231°C	Dielectric	20
	232°C	235°C	Expansion	20
Cooling	212°C	226°C	Expansion	21
	219°C	230°C	Expansion	20
		228°C	Dielectric	20

ZrO_2 sample at 950°C produces only $PbZrO_3$ and tetragonal ZrO_2. Further heating of this mixture causes the tetragonal ZrO_2 to transform to monoclinic ZrO_2 and the diffraction lines of $PbZrO_3$ to become more defined.[27] Studies involving mixtures rich in PbO do not report the existence of $2PbO \cdot ZrO_2$.[16,28] The phase diagram[26] showing the incongruent melting of $PbZrO_3$ is given in Fig. 3.

Single crystals of $PbZrO_3$ produced by evaporation at 1250°C with a $PbCl_2$ flux are light brown cubes and octahedra up to 0.3 mm in length.[29]

$PbZrO_3$ is reported to decompose at approximately 1150°C.[16] The term decompose must refer to the sublimation of PbO, leaving ZrO_2.

Further discussion on the domain properties, antiferroelectric and ferroelectric theory and other physical properties for both $PbZrO_3$ and $PbTiO_3$ are summarized in Ferroelectric Crystals by Jones and Shirane.[30]

C. Mixtures of $PbTiO_3$ and $PbZrO_3$

$PbTiO_3$ and $PbZrO_3$ have been shown to possess the cubic perovskite structure above their respective Curie points. Since they differ in structure only by the substitution of zirconium for titanium, it would be expected that a complete solid solution exists above the Curie point. This, indeed, appears to be true up to 900°C where the lattice parameter vs $PbZrO_3$ content still follows Vegard's Law.[31] High temperature X-ray studies above 900°C have not been attempted due to the rapid loss of PbO vapor.

Substitution of the zirconium ion for the titanium ion in the $PbTiO_3$ lattice results in a decrease in the Curie temperature.[7,32]

Below the Curie temperature two morphotropic boundaries exist. For compositions rich in $PbTiO_3$ a tetragonal phase exists; from about 47 mole % $PbTiO_3$ to nearly 8 mole % $PbTiO_3$ the phase is rhombohedral;

near $PbZrO_3$ the orthorhombic phase is the stable one. The Curie temperature vs composition curve (the upper curve in Fig. 4) has been established by dielectric constant and linear expansion measurement.[7,33] It should be noted that this figure violates the phase rule. The phase fields present should be separated by a two-phase region at the boundary between the tetragonal and rhombohedral transition. The antiferroelectric region A_β is probably a two phase region extending about the line separating F_α and A_α; in this case one phase would be ferroelectric while the other would be antiferroelectric.

The region near the rhombohedral-tetragonal transition shows the highest electromechanical coupling coefficient and piezoelectric modules (d_{33}).[16,34,35] For this reason, several studies have attempted to determine the location of this boundary. The results are given in Table III.

The orthorhombic phase, extending from $PbZrO_3$ to about 8 mole % $PbTiO_3$ at room temperature is antiferroelectric; its c/a tetragonality ratio is less than one. Ferroelectricity is exhibited, however, by both the rhombohedral and tetragonal phases. At room temperature c/a = 1.06 for $PbTiO_3$ and decreases to c/a = 1 for 8 mole % $PbTiO_3$. As the tetragonality ratio decreases upon the replacement of zirconium for titanium ion, the unit cell volume increases from a low value of 62.72Å^3 for $PbTiO_3$ to 70.23Å^3 at 7.5 mole % $PbTiO_3$.[7]

As reported earlier, loss of lead oxide results in compositional changes during high temperature property measurements and single crystal growth. Sublimation of PbO from PZT composition is negligible below approximately 800°C.[14] For a given temperature above 800°C higher rates of loss are seen as the $PbZrO_3$ content increases.[37]

TABLE III. Values for the composition of the tetragonal-rhombohedral boundary.

Composition $\frac{PbZrO_3}{PbZrO_3 + PbTiO_3}$	Reference
0.53 ± 0.01	35
0.54 ± 0.005	16
0.55 ± 0.25	34
0.55	36

Fluorescent analysis of the surface of a PZT sample which has lost weight suggests that a small amount of Ti may be lost in addition to the PbO.[37]

The loss of PbO can be minimized by muffling with a composition richer in $PbZrO_3$.[37] For example, a $PbZrO_3$ pellet will provide this atmosphere for all other PZT compositions. Samples subjected to this treatment can actually gain weight.

Attempts to grow single crystals of lead zirconate titanate have used a flux of PbO and B_2O_3 to obtain crystals containing only a few mole % $PbZrO_3$.[38] Preliminary studies with a mixture of KF and PbF_2 as a flux have yielded crystals of various compositions.[39] In most studies the use of polycrystalline samples still predominates.

A lead zirconate titanate (PZT) piezoelectric sample of a particular composition is usually made by mixing together the proper proportions of PbO, TiO_2 and ZrO_2, although a co-precipitation process[40-42] and the use of $Pb(CO_3)$ and $Pb(OH)_2$ have been explored.[43]

X-ray examination of a mixture of PbO, TiO_2 and ZrO_2 in the molar ratio of 2:1:1 heated to different temperatures for a given period of time reveal the following unbalanced reactions:[44]

(1) $PbO + TiO_2 \rightarrow PbTiO_3$

(2) $PbTiO_3 + PbO + ZrO_2 \rightarrow Pb(Zr_{1-x}Ti_x)O_3 \quad X < 0.5$

(3) $Pb(Zr_{1-x}Ti_x)\ O_3 + PbTiO_3 \rightarrow Pb(Zr_{0.5},\ Ti_{0.5})O_3$

The first reaction is almost complete after heating at 650°C for two hours. At approximately the same temperature the second reaction begins. Apparently, the $PbTiO_3$ immediately begins to form a $PbZrO_3$ rich solid solution when PbO and ZrO_2 start reacting. Whether the lead oxide and

zirconia first react to form $PbZrO_3$ is not known; however, $PbZrO_3$ is not detected at any time. After two hours at 750°C the uncombined PbO and ZrO_2 are almost consumed, but some $PbTiO_3$ still remains. Finally, the $Pb(Zr_{0.5}, Ti_{0.5})O_3$ solid solution is formed by consuming the unreacted $PbTiO_3$.

These reactions seem reasonable in light of the relative stabilities of $PbTiO_3$ and $PbZrO_3$. If equimolar mixtures of TiO_2 and $PbZrO_3$ are heated, the $PbZrO_3$ will decompose leaving ZrO_2 and $PbTiO_3$ (with 7 mole % $PbZrO_3$ in solid solution). Conversely, if a similar experiment is performed with $PbTiO_3$ and ZrO_2 the result is ZrO_2 containing a small amount of TiO_2 in solid solution and $PbTiO_3$ containing a small amount of $PbZrO_3$.[35]

A reaction diagram in the ternary system $PbO\text{-}ZrO_2\text{-}TiO_2$ prepared from X-ray studies of samples of various compositions that were heated at 1100°C for one to two hours is shown in Fig. 5.[16,35] Of particular interest here is the section with a constant molar ratio of $\frac{PbO}{ZrO_2+TiO_2} = 1$. The solid solution region about this molar ratio extends from 0.96 to 1.08 as determined by phase studies and lattice parameter variations. Therefore, it is concluded that a small loss or gain of PbO from a PZT sample during processing should not cause a new phase to form, providing the loss is uniform throughout the sample, not just at the surface.

Very recently the ternary system $PbO\text{-}TiO_2\text{-}ZrO_2$ was examined by quenching methods followed by X-ray analysis.[26] In the region containing more than 50 mole % PbO the tie lines between the liquid and PZT solid solution were determined for 1100°C, 1200°C, and 1300°C. At 50 mole % PbO the composition-temperature diagram showed the three phases, liquid + ZrO_2 + $Pb(Zr, Ti)O_3$, to be in equilibrium for a temperature interval

above 1340°C and for compositions containing more than 14 mole % of $PbZrO_3$, (Fig. 6). Further heating would cause the PZT to melt which would leave only ZrO_2 + liquid as the equilibrium phases. A proposed polythermal projection was also given, (Fig. 7). The authors concluded that the vertical section at 50 mole % PbO is not a quasi binary. (Appendix II).

This fact complicates the analysis of the $PbZrO_3$-$PbTiO_3$ system because the equilibrium criterion used in determining binary phase diagrams no longer applies. A greater reliance on experimental data is therefore necessary.

Quenching procedures are not entirely satisfactory in a complex oxide system, and the results must be substantiated by other independent methods. Determination of the solidus temperature depends upon the detection of a liquid phase which may be found by quenching in the liquid phase or by the nucleation and growth of nonequilibrium phases resulting from resolidification. If the liquid rapidly reacts with the solid phase on cooling, a greater amount of liquid is necessary for detection by either optical or X-ray methods. The small amount of liquid formed at the solidus point would react rapidly with the solid on cooling to room temperature and would not be detectible. A new phase cannot be detected until a sufficient amount of liquid is formed so that on cooling not all of the liquid has time to react with the solid. The effect is to raise the solidus temperatures determined by quenching. Even more important, the phases detected after quenching the melt may have little relationship to the equilibrium situation. Assuming the liquid phase cannot be quenched to room temperature, as the aforementioned study indicated, the following problem can arise. On cooling a homogeneous melt, a

non-equilibrium species may preferentially nucleate because of lower surface energy considerations. If the reaction between the nucleated species and the remaining melt is sufficiently slow, due either to slow diffusion in the solid or the presence of a reaction layer, the solid obtained by quenching the liquid will not represent the situation in the liquid region.

The most sensitive method that should be used in conjunction with quenching techniques is thermal analysis; this and other potential high temperature phase study methods are discussed in the next section.

D. Possible Methods of Investigation

Several methods are available for high temperature phase equilibrium studies. These methods include thermal and differential thermal analysis, high temperature X-ray and optical microscopy techniques, vapor pressure and quenching studies. Not all of these are applicable to this system. The primary complication develops from the PbO sublimation at higher temperatures.

High temperature X-ray analysis detects only the phases present within a few microns of the surface in the PZT system because of the high scattering of the Pb and Zr ions. As lead oxide is lost from the surface, the phases detected would not be indicative of the composition of the sample. The high temperature X-ray camera is then unsatisfactory above approximately 900°C.

Observation of the melting point by optical methods is also hindered by the loss of PbO. The sample is obscured from view by the condensation of lead oxide on the glass window of the heating stage. The loss of PbO from the small amount of powder usually used (< 1 gm) would cause a radical change in composition even if the specimen were observable.

Differential thermal analysis is useful for detecting reactions taking place in the solid state. Precise determination of the reaction temperatures, particularly the melting point, is hindered by the prior sintering of the powder. Before the onset of sintering the powder is in direct contact with the wall of the differential cell. The temperature of the powder is then close to that of the block since the major mode of heat transfer is conduction. Sintering causes a shrinkage of the powder away from the cell wall resulting in a larger temperature gradient between the block and the powder. DTA was used here to examine the possibility of reactions taking place below the solidus temperature, but not for the determination of this temperature.

Equilibrium vapor pressure studies are useful for the detection of high temperature phases. A convenient method is a Knudsen cell weight loss experiment, providing the vapor pressure is less than 10^{-3} atmosphere in the temperature range of interest. This method was employed.

Quenching methods were discussed earlier.

Thermal analysis is generally the most rapid method for determining phase transitional temperatures, providing the heat of transition is sufficient for detection and that the reaction is not very sluggish. This is generally true for reactions involving solid-liquid transitions. Determination of the transition temperatures found in this study was by this method.

II. EXPERIMENTAL PROCEDURE

A. Preparation of Lead Zirconate Titanate

Powders containing various ratios of $PbTiO_3$ to $PbZrO_3$ were made in batches by weighing the proper proportions of reagent grade PbO, TiO_2 and ZrO_2 (Table IV) into a glass mixing jar. The powders were thoroughly mixed with isopropyl alcohol and vacuum dried. Following the drying procedure, the powders were pressed into 1 inch × 1/2 inch pellets, placed in a Pt. crucible and calcined at 800°C for an average of 229 hours. The pellets were crushed into powder that would generally pass through a 200 mesh screen. A spectographic analysis of powders prepared by this method did not detect an increase in the impurity content.

X-ray examination of the finished powders showed only the PZT phase to be present. The samples were also checked by chemical analysis to insure the correct composition.

B. Chemical Analysis

The calcined samples were analyzed for Ti, Zr and Pb using wet chemical methods. The powders were taken into solution by pyrosulfate fusion and mixed with HCL to form zirconium and titanium chloride complexes.

Ti analysis:[45] The above solution was mixed with concentrated H_2SO_4, heated until H_2SO_4 fumes were detected, cooled and passed through a filter to remove $PbSO_4$ precipitate. The filtrate was mixed with a hydrogen peroxide solution to form a titanium peroxide complex. The concentration of titanium was finally determined by optical density readings at 420 mμ on a spectrophotometer.

TABLE IV. Results of semiquantitative spectrographic analysis on the reagent grade oxides used.

	PbO (Baker's reagent grade)	TiO_2 (Fisher's reagent grade)	ZrO_2 (Wah Chang reactor grade)
Si	0.004%	0.2%	0.003
Mg	.005	.001	.002
Fe	< .002	.01	.01
Al	.002	.04	.005
Ca	.001	.002	.005
Cu	.0005	--	--
Ba	.002	--	--
Bi	.01	--	--
Hf	--	--	< .025%
Ag	<.0005	--	--
Nb	--	--	.05
Ti	--	--	.005
Y	--	--	.006

Zr analysis:[46a] Aliquots of the original solution were diluted and heated to near boiling. The zirconium and titanium were precipitated as hydroxides by bubbling NH_3 into the solution. The precipitates were collected in a filter while the filtrate containing the lead ion was discarded. The precipitates were brought back into solution by mixing with 50% HCL and heating. Zirconium was selectively precipitated as zirconium tetramandelate by mixing the solution with mandelic acid. The precipitate was collected by filtering and fired at 1000°C. The residue was then weighed as ZrO_2.

Pb analysis:[46b] A separate sample was dissolved by pyrosulfate fusion and then mixed with concentrated HNO_3 and Cu (to form $Cu(NO_3)_2$). The solution was maintained at 90°C while PbO_2 was plated out on a circular Pt gauge electrode. After the plating process, the electrode was dried and weighed.

Results of the chemical analysis are summarized in Table V, with the weight percent figures representing the average of three determinations per PZT composition.

C. X-ray Analysis

All X-ray identification was by powder diffractometry with CuK_2 radiation. The PZT peaks were identified by comparing the 2θ values of the observed peaks with the 2θ values calculated from crystallographic data.[34] For the determination of interplanar spacings, the diffractometer was first calibrated with a polycrystalline quartz standard. The scanning speed was 1/8°/min.

Care must be taken in the identification of low concentrations of zirconia because several $CuK\beta$ lines of PZT are at the same two theta

TABLE V. Chemical analysis results of lead zirconate titanate powders

Mole % PT / Wt %	10	20	30	40	60	65	70	75	80	85	90	95
% TiO_2	2.52	4.85	7.28	9.905	14.61	16.35	17.04	18.50	19.76	20.88	23.58	24.84
% ZrO_2	32.26	28.90	26.01	22.32	15.45	13.67	11.74	9.88	7.99	4.91	4.07	2.025
% PbO	66.1	66.0	66.6	67.5	69.8	70.55	71.1	71.95	72.25	72.53	72.9	73.45
Closure	100.9	99.75	99.9	99.73	99.9	100.6	99.9	99.8	100.0	98.3	100.6	100.3
Mole % PT*	10.74	20.56	30.16	40.64	59.33	64.85	69.13	74.29	79.23	86.77	89.94	94.99

* Mole % $PbTiO_3$ calculated on the basis that all TiO_2 is combined in $PbTiO_3$ and all ZrO_2 is combined as $PbZrO_3$ and that their total = 100.0%.

value as the most intense line of ZrO_2. This problem was eliminated by sufficient Ni filtering or with a monochromator.

D. Thermal Analysis

A large cylindrical furnace with an outside water cooled steel jacket insulated from the heating zone by high temperature bricks was used (Fig. 8). $MoSi_2$ elements arranged in a circular manner provided heat. Down the center of the furnace was an Al_2O_3 muffle tube closed at both ends with removable bricks.

Temperature was regulated by a variable proportional drive controller with the control thermocouple approximately 1" from one of the elements midway between the top and bottom of the heating zone. The constant heating zone of this furnace was 2-1/2" long.

To insure little heat loss away from the sample container, the Pt crucible was suspended from a Pt wire (Fig. 9). The conical container was placed in a loop of Pt wire hanging from a small piece of alumina tubing. The alumina tubing was threaded through with a second Pt wire that led up a thermocouple tube insert in the brick plug. This arrangement allowed removal of the sample from the furnace by merely taking the brick plug from the furnace.

Powders of the composition to be tested were weighed (30 gm) into the platinum crucible and a piece of 0.001 inch Pt foil was spot welded over the top to reduce the vapor loss at high temperatures. A 8 mil Pt and 90% Pt + 10% Rh thermocouple insulated with a 25 mil Al_2O_3 tubing was inserted into the thermocouple well at the crucible's bottom. The thermocouple was secured in place by first notching the alumina tubing at the correct distance from the bead to insure contact with the top of

the thermocouple well. The notch was then wrapped with Pt wire. After insertion into the well, the bottom of the well was pinched shut below the Pt wire.

The system was calibrated with reagent grade Na_2CO_3 (mp 851°C)[47] and $CaO.B_2O_3$ (mp 1162°C)[48] which was obtained from the Bureau of Mines Pacific Experiment Station. Agreement was within 3°C. The value obtained for the melting point of $PbTiO_3$ was in excellent agreement with published temperatures (1281 and 1285°C) and was also used for calibration purposes. The sensitivity of the apparatus was demonstrated by its ability to detect the Curie point transition of $PbTiO_3$.

Temperature was monitored by a potentiometrically balanced strip chart recorder used with a cold junction. Before each run the electronics of the system was checked against a known millivolt source.

A typical run would commence when the brick plug holding the crucible was inserted into the furnace held at approximately 1250°C. After holding for approximately 10 minutes to homogenize the powders, the temperature of the furnace was raised at a constant rate. The holding period was short to prevent as little PbO loss as possible. After the sample melted completely the temperature was held constant for approximately 5 to 10 minutes. Following the hold period, the temperature was driven down at a constant rate to about 1250°C. After removing the crucible from the furnace, the crucible was weighed to check weight loss. The weight loss was generally less than 1% of the total weight of the charge. The solid was removed from the crucible by chipping with a cold chisel and hammer; it was examined later by X-ray analysis.

Additional tests to confirm the solidus temperature were performed by placing a sealed 7 mm x 35 mm Pt crucible containing PZT powder into a furnace held at a constant temperature. A thermocouple in contact with the outside of the crucible was used for temperature determination. The charge was examined for liquid formation after quenching in liquid nitrogen following a 30 min. soak at a constant temperature.

E. Differential Thermal Analysis

Differential thermal analyses (DTA) were conducted in a Pt cell, a rectangular block containing two cylindrical cavities.[49] The differential thermocouple was placed into each cavity through a hole drilled midway between the top and bottom of the cavity. A Pt and 90% Pt-10% Rh thermocouple was placed into the center of the block for temperature monitoring. The furnace was regulated by a variable-proportional drive controller-recorder system. The control thermocouple, independent of the DTA cell, was located near the Pt wound core that surrounded the DTA cell.

Alumina was used as the reference material.

F. Vapor Loss Studies

Weight loss experiments were conducted in vacuum with the weight change recorded continuously on an automatic recording microbalance.

A Kanthal wound muffle furnace was placed around a 2" O.D. mullite tube which was sealed at both ends with O ring seals and brass fittings. Above the mullite tube a tee-shaped copper tube connected the mullite tube to the vacuum system and the microbalance, (Fig. 10).

Regulation of temperature was by a variable proportional controller, using a control thermocouple placed at the hottest point between the furnace wall and the mullite tube. The isothermal zone was 1-1/2 inches

long. The sample temperature was obtained by an optical pyrometer that was sighted through a glass window in the brass fitting at the bottom of the mullite tube.

The sample hung from a Pt wire connected to one arm of the microbalance and was counterbalanced by weights on the other pan. The capacity of the balance was 400 mg.

Wt. loss runs were begun by lowering the sample into the furnace which was at constant temperature; the system was then evacuated. The sample was estimated to be in equilibrium with the surroundings within 5 minutes after the vacuum was applied. Following the vacuum treatment air was admitted to the furnace and the sample removed.

III. RESULTS AND DISCUSSION

A. Investigations Below the Solidus Temperature

1. DTA

To establish whether a high temperature phase exists, differential thermal analysis was undertaken to detect any heat effect associated with a possible phase change. The powders investigated were mainly those in the composition range between 47.5 and 100 mole % $PbTiO_3$. This range was the most likely region as indicated by thermal analysis. The results showed only two endothermic reactions correcpsonding to the Curie and melting point, respectively (Fig. 11). Several tests on the $PbZrO_3$ rich side region indicatedthe same results.

2. X-Ray Studies

A supplement to DTA studies was performed by mixing calcined powders of different composition in 50-50 mole % mixtures. The powders were fired for 1 hour, quenched in liquid nitrogen, and then examined by X-ray analysis. The results are listed in Table VI. A typical X-ray diffractometer pattern of the mixture before and after firing is shown in Fig. 12.

These results show that there is no tendency for a given mixture to separate into a new compound other than that formed by the mechanical mixture. This conclusion could possibly be criticized on two grounds. First, the high temperature phase may not be quenched to room temperature. Second, the only proper method of determining the presence of a high temperature phase is by the use of a high temperature X-ray camera. In answer to the quenching question, even though the phase does not quench to room temperature the time to recombine to the correct mixture composition

TABLE VI. Results of heating for 1 hour of equimolar mixtures of various compositions.

Mixture 50/50 mole %	Temp	Resultant composition
$PbZrO_3$+$Pb(Zr_{0.80},Ti_{0.20})O_3$	1254°C	$Pb(Zr_{0.90},Ti_{0.10})O_3$
$Pb(Zr_{0.90},Ti_{0.10})O_3$+$Pb(Zr_{0.30},Ti_{0.70})O_3$	1281°C	$Pb(Zr_{0.40},Ti_{0.10})O_3$
$Pb(Zr_{0.60},Ti_{0.40})O_3$+$Pb(Zr_{0.10},Ti_{0.90})O_3$	1252°C	$Pb(Zr_{0.25},Ti_{0.75})O_3$
$Pb(Zr_{0.70},Ti_{0.30})O_3$+$PbTiO_3$	1254°C	$Pb(Zr_{0.45},Ti_{0.75})O_3$

is probably insufficient. A splitting of the diffraction peaks would be expected. No such splitting is seen. The idea of using a high temperature camera above 900°C is not valid since the depth of penetration of the X-rays is very small due to the large scattering of the lead and zirconium ions. Above 800°-900°C the loss of vapor becomes important; therefore, the surface of the sample is not indicative of the interior.

A sample heated to just below the solidus temperature, held for one hour and quenched in liquid nitrogen shows only the original calcined mixture with no line splitting.

At 900°C the lattice constant has been shown to obey Vegart's Law.[31]

The conclusion is that the phase below the solidus is a solid solution with the cubic perovskite structure.

A rapid method of determining the composition of a powder is to find the d spacing of either the {321} or {211} lines. These lines are chosen because of their relatively strong intensity. Figures 13, 14 and 15 show the comparison between the d values calculated from the lattice parameters (solid line) and those obtained by diffractometer measurements. (circles). The lattice parameters were obtained from a National Bureau of Standards report.[34] The parameters were assumed to vary linearly over the composition range and were fitted to a straight line by a least means square procedure. Interplaner spacings were calculated from the data using a digital computer. Appendix 1 summarizes the results.

In order to obtain good agreement with the calculated values, it was necessary to treat the calcined powders at 1200°C for 1 hour in a closed Pt crucible. This treatment homogenizes the calcined powders which still show a variation of composition after calcining for 200 hours at 800°C. Figures 16 and 17 represent diffractometer patterns

for step scanning and continuous scanning, respectively. In both drawings the upper figure is the calcined material and illustrates the inhomogeneity in the powder by the broad ill-defined peak. After the 1200°C treatment the peaks are easily resolved. A conclusion to be drawn from this is that the uniformity of start powders for various processing studies is achieved only by reheating the calcined powders to higher temperatures. The common practice of calcining the mixed oxides for 1 hour at 800-900°C is therefore insufficient for the attainment of reproducible starting powders.

3. Weight Loss Studies

It was hoped that discontinuities in the log vapor pressure vs composition plot would also show whether an undetected high temperature phase did exist. This hope was not realized because of incongruent vaporization taking place in vacuum, demonstrated by X-ray examination of the sample's surface.

During the weight loss runs the PZT phase is not the only one present. The phases present in vacuum are summarized in Table VII. Furthermore, the vapor pressures at 1050°C and 1100°C proved to be outside the Knudsen cell range if PbO is assumed the vapor species.

The results are compatible with the reaction diagram in Fig. 5. For example, the phases present after PbO loss from the $Pb(Ti_{0.95}, Zr_{0.05})O_3$ composition are solid solution TiO_2 and 95 mole % $PbTiO_3$. If a line of constant mole ratio of $ZrO_2/TiO = .95$ is drawn on the reaction diagram, the stable phases become TiO_2 and PZT as PbO is lost. Similar arguments can be proposed for the other compositions. Although the agreement is not exact the trend is good. The appearance of other phases after a small percent weight loss depends on whether the experiments

TABLE VII Phases detected after sublimation of lead oxide in vacuum

Mole % $PbTiO_2$	Phases present after wt. loss in vacuum	Approximate % loss
95%	Anatase (TiO_2), rutile TiO_2, 95% PZT	5%
90%	Anatase (TiO_2), rutile TiO_2, 95% PZT	3%
85%	$ZrO_2 \cdot TiO_2$, rutile, PZT	7.6%
85%	Trace ZrO_2? ZrO_2TiO_2, rutile PZT	20%
85%	(cooled in vacuum)	
	ZrO_2?, $ZrO_2 \cdot TiO_2$, rutile, PZT	18%
75%	$ZrO_2 \cdot TiO_2$, PZT	—
47.5%	ZrO_2, rutile, $ZrO_2 \cdot TiO_2$, PZT	21%
30%	ZrO_2, PZT tetrag. ($ZrO_2 \cdot TiO_2$ or PZT rhomb)	23%

are conducted in vacuum or air. If approximately 1% of the total weight is lost in air the PZT phase is still present, but if the same percentage is lost in vacuum, additional phases appear. (Fig. 18) Exposure of the sample to air at the same temperature would cause the PZT phase which had disappeared to reappear (Fig. 19).

A tentative explanation for this phenomena follows: As PbO is lost from the surface, the composition of the surface will move along a line of constant mole ratio of ZrO_2/TiO_2 towards the TiO_2-ZrO_2 binary on the ternary diagram.

The phases present will depend upon wehther a depletion layer is formed. If the diffusion of PbO to the surface is slow, the phases detected by X-rays will be mainly those lying off the line of 50 mole % PbO since the composition of the surface would rapidly lose PbO and other phases would appear. In vacuum the rate of PbO loss from the surface is fast, whereas in air the rate of removal of PbO vapor from the sample is much slower due to the presence of a gas above the surface. Therefore, the time required to lose a given weight in vacuum is shorter than the time necessary to lose the same amount in air. The longer time in air allows diffusion to replenish the surface with PbO and yields a surface that more nearly reflects the average composition of the solid; then new phases are not detected until a larger percentage of PbO is lost.

Vacuum weight loss results in the formation of a depletion layer which is verified by the appearance of new phases. Treating a vacuum sample in air allows the PbO to redistribute in the solid. For the surface, this means moving on a line of constant Zr/Ti ratio towards the PbO vertex of the ternary diagram. A sufficient amount of PZT will reform, by reaction of the PbO with the TiO_2 and ZrO_2 present at the

surface, and be detected again by X-ray analysis.

The effect air has on the sample could also be explained by the oxidation of the divalent lead ion to its tetravalent state. As a result, a lead ion vacancy would be created. This would enhance the lead ion mobility in an air atmosphere. In vacuum the vacancy concentration would decrease and a depletion layer would form. The reaction $2Pb^{2+} + 1/2\ O_2 \leftrightharpoons Pb^{4+} + PbO + \square$ has been reported to take place in the PZT system.[50]

In either case, the results are explained by a deficiency of PbO near the surface which results in the appearance of other phases.

B. Investigations Above the Solidus Temperature

1. Thermal Analysis of $PbTiO_3$ and $PbZrO_3$

The melting point of $PbTiO_3$ was found to be 1286°±3°C by thermal analysis; the horizontal plateau on both the heating and cooling curves was taken as the melting point. Close examination of the heating curve shows a slight melting interval (~ 3°C) rather than a very well defined plateau. This rise could indicate a peritectic reaction where $PbTiO_3$ decomposes to PbO rich liquid and TiO_2 rich solid, or impurities in the sample. Heating curves of Na_2SO_4 and NaCl also show this type of behavior with a heating interval as great as 60°C.[51] The melting of $PbTiO_3$ produces an unusually level thermal arrest by these standards.

To check this point three crucibles were held for 30 min. at 1280°C, 1282°-1283°C, and 1286°C, respectively. The first one showed no sign of liquid formation. At 1283°C some liquid formed, while at 1286°C the material had completely melted. In view of the recent claim of a eutectic reaction in the titania rich region of the PbO-TiO_2 system,[15]

the melting interval is assumed to be due to impurities. $PbTiO_3$ is then a congruently melting compound. Combining the melting point data with the data available from the literature, a binary diagram containing two eutectic reactions, one on either side of $PbTiO_3$, is proposed (Fig. 20).

The determination of the melting point of $PbZrO_2$ was not so successful. Continued heating to 1550°C gives no indication of melting and results only in severe deterioration of a platinum crucible. Above 1200°C the vapor pressure of PbO becomes appreciable. The solid remaining after heating to 1550°C is monoclinic zirconia.

To circumvent the problem of PbO loss, several crucibles were inserted into the furnace, which was already at a constant temperature, and held for 5 minutes. It was hoped that liquid formation would be noted before all the PbO vaporized. No liquid was detected by visual inspection. The solid that remained, as determined by X-ray analysis, contained $PbZrO_2$ in the center with a white layer of ZrO_2 on the outside. Above 1500°C the crucible is so severely attacked that experiments cannot be conducted. For instance, Fig. 21 shows a Pt crucible containing $PbZrO_3$ before firing and after firing at 1520°C for 3 minutes.

The onset of attack appears very suddenly as the furnace temperature is raised. If the reaction

$$PbO_{(vap)} + Pt \rightarrow Pt\ (Pb)\ solution + 1/2O_2$$

were taking place a sudden increase in the PbO vapor pressure would cause an acceleration of this reaction. This sudden increase could be explained by a peritectic decomposition reaction.

$$PbZrO_3 \rightarrow liquid\ (rich\ in\ PbO) + ZrO_2(S.S.)$$

The vapor pressure would be near that of the boiling point (1472°C) of PbO.

From these observations the report of a melting point temperature of 1570°C seems erroneous. The idea of a peritectic reaction where $PbZrO_3$ decomposes to a solid rich in ZrO_2 and a liquid rich in PbO agrees basically with the present results, but the determination of the exact temperature seems impossible.

The possibility of a compound $2PbO\ ZrO_2$ was investigated. Mixtures of $2PbOZrO_2$ were heated at 800°C for a total of 54 hours. At 18 hour intervals the sample was ground by mortar and pestle and analyzed by X-ray diffraction. The powder was replaced in the crucible and the heat treatment continued. This operation was repeated two times. The only phases detected were $PbZrO_3$ and orthorhombic PbO (massicot).

As a result, the phase diagram in Fig. 3 appears to be reasonable.

The vertical section at 50 mole % PbO in the $PbO\text{-}ZrO_2\text{-}TiO_2$ composition temperature diagram cannot be a quasi binary if $PbZrO_3$ melts incongruently.

2. Thermal Analysis of Lead Zirconate Titanate Mixtures

The final temperatures used for the phase diagram were obtained from data derived from heating curves analysis. The cooling curves proved to be inaccurate and were useful only in indicating the general trend of events.

Cooling curves for a complex oxide system are unreliable for the determination of either the liquidus or solidus temperatures. Supercooling, preferential nucleation of a non-equilibrium solid, and low diffusion rates in the solid can cause substantial errors in the temperature determination.

The first inflection points on the temperature-time curve (Figs. 22,23) observed on cooling suggests supercooling when compared with the liquidus temperatures obtained from heating curves. A slight increase in temperature, definitely indicating supercooling, is noted after the first inflection point for 100, 95 and 90 mole % $PbTiO_3$ compositions. At compositions richer in $PbZrO_3$ the first inflection point appears to split into two. The second point could be due to the peritectic reaction which is shown in Fig. 6. The cooling curves of a peritectic arrest in metals generally are characterized by pronounced undercooling and very short isothermal arrest which slowly merges into the cooling rate of the furnace.[52] A peritectic reaction in the $PbTiO_3$-$PbZrO_3$ would be expected to show a similar behavior.

The final inflection point near the melting point of $PbTiO_3$ is due to microsegregation known as "coring." Coring is particularly common when dendrite growth is present. The composition of the core of the dendrite is different from the outside of the dendrite.[52]

The melt of a given PZT composition (vertical line) will begin to solidify on reaching the liquidus temperature and deposit a solid with a composition in equilibrium with the liquid at that temperature. As the temperature is lowered the average composition of the solid is not that indicated by the solidus line due to slow diffusion in the solid, but is richer in $PbZrO_3$. The deviation from the equilibrium composition increases as the temperature is lowered. Upon reaching the equilibrium solidus temperature for the specific composition the average solid composition is still rich in $PbZrO_3$ and liquid rich in $PbTiO_3$ remains. Cooling further, the average solid composition finally coincides with the original composition and the liquid rich in $PbTiO_3$ solidifies.

Support of this hypothesis is indicated by the different solidus temperatures obtained for different cooling rates. The faster the cooling rate, the shorter the period of time for solid state diffusion to take place; therefore, the larger the deviation of the average solid composition from equilibrium and the lower the final freezing temperature. Examination of Table VIII indicates the final inflection points of the 5.6°/min cooled runs to be lower in temperature than the 2.8°/min runs. Observation of the melt shows dendritic growth to be present which appears to decrease with addition of $PbZrO_3$.

Table VIII and Fig. 24 summarize the cooling data.

Examination of the solid taken from the crucible shows the following: Compositions containing 90, 95 and 100 mole % $PbTiO_3$ yield only the original composition as ascertained by X-ray analysis. At lower percentages of $PbTiO_3$, ZrO_2 (monoclinic) and PbO (orthorhombic and tetragonal) were present in addition to the PZT phase. The PZT phase was generally richer in $PbTiO_3$ than the original composition. A cross-section of a crucible containing a solidified melt whose original composition was greater than 15 mole % $PbZrO_3$ would have a greenish-white top layer followed by a gradual transition to a brownish-orange solid along the sides and bottom of the crucible. The phases present on the top layer are PZT and ZrO_2, while in the bottom the same species were detected with the addition of PbO.

The solids found at the bottom and sides of the crucible would be the phase to first solidify on cooling, while those at the top would be the last. The last solids to solidify are PZT and ZrO_2. The detection of PbO at the bottom of the crucible shows that the liquid at high temperatures is rich in PbO since it is still unreacted after

TABLE VIII. Summary of cooling curve analysis

Composition mole % $PbTiO_3$	Cooling rate	Upper temp. °C		Lower temp. °C
0	3.5	1287		—
0	8	1290	SC	—
5	2.8	1305	SC	1290
5	5.6	1302	SC	1288
10	2.8	1329	SC	1290
10	5.6	1326	SC	1286
15	2.8	1335	1333	1293
15	5.6	1330	—	1288
20	2.8	1340	1335	1289
20	5.6	1335	1325	1285
25	2.8	1347	1340	1289
25	5.6	1345	1336	1279
30	2.8	1354	1342	1231
30	5.6	1355	1345	ND
35	2.8	1359	1347	ND
35	5.6	1362	1345	ND
40	2.8	1365	1352	ND
52.5	2.8	1398	1372	ND
60	2.8	1410	ND	ND

ND - Not detectable

SC - Supercooling

cooling. The appearance of unreacted ZrO_2 in the presence of PbO seems odd considering the solid state reaction to form $PbZrO_3$ that takes place when powders of PbO and ZrO_2 are mixed and heated. This could be possible if the ZrO_2, PZT, and liquid (rich in PbO) phases are in equilibrium at some temperature above the solidus. Alternatively, since the phases present do not react rapidly once in the solid state, the same situation could be caused by nucleation of ZrO_2 and PZT followed by solidification of the remaining melt. Once in the solid state the reactions necessary to homogenize the sample back to the original composition could be very slow.

From this discussion it is evident that the temperatures determined by cooling curve analysis must not be used because of the inhomgeneity of the final solid. Also, the phase equilibria existing at high temperatures cannot be determined by cooling curves or quenching methods alone. Resolution of the question of whether three phases exist at high temperatures or preferential nucleation causes the observation of PbO, PZT and ZrO_2 at room temperature can only be solved by heating curve analysis because of the absence of nucleation and growth considerations.

The heating analysis should be particularly sensitive to phase changes in powders by the thermocouple arrangement used here. The thermocouple accounts for only the portion of charge immediately surrounding it. When this portion melts, a break in the heating curve will result. As heating proceeds, sintering takes place causing a shrinkage of the powder away from the crucible wall. This is demonstrated by the rattling of the unmelted charge in the crucible after heating near the melting point. The charge is then in contact with the top of the thermocouple well which is supporting the sintered powder. For

this reason the crucible-thermocouple arrangement should be very sensitive to melting. The first inflection point in the heating curve would then represent the solidus temperature (Figs. 25-27).

To check the solidus temperature, the furnace was held near the indicated solidus temperature, but lower than the second inflection point. A small Pt crucible sealed with annealed Pt foil and held down by an inverted Al_2O_3 crucible was lowered into the furnace and held for 1/2 hour. The crucible was quenched in liquid nitrogen and examined for liquid formation. This technique was used for a series of compositions shown in Table IX. Figure 28 shows one such result. In all cases liquid formation was noted, thus supporting the hypothesis that the first inflection point represents the solidus point.

Continued heating causes a second inflection which shows a larger heat effect. This is rationalized in the following manner: The sample sinters to a conical shaped solid supported by the thermocouple well and partially separated from the wall of the crucible. Heat transfer to the solid is by convection through the gas phase present in the crucible and conduction along the solid thermocouple well. The hottest point of the solid is the top of the thermocouple well because good contact between the sintered powder and Pt crucible is maintained in this region. After the first inflection point is reached the liquid formed in the vicinity of the thermocouple is very small and therefore shows a small heat effect. Further heating plus the added heat conduction effect of the liquid formed brings the remaining solid (major mass) to the solidus temperature or above it. When this mass melts and slumps down into the crucible the second inflection point is noted and slight cooling takes place near the thermocouple because of the heat drawn

TABLE IX. Summary of constant temperature heat treatment

Composition mole % $PbZrO_3$	Constant temp.	Appearance of charge at 30 min.
0	1281°C	Solid
0	1282-3°	Small amount of liquid formed
0	1286°	Melted
5	1280°	Solid
5	1294°	Small amount of liquid formed
20	1310°	Solid
20	1325°	Small amount of liquid formed
20	1324°	Small amount of liquid formed
40	1335°	Solid
40	1343°	Small amount of liquid formed
40	1356°	Liquid + solid
52.5	1362°	Small amount of liquid formed
52.5	1369°	Liquid + solid
60	1379°	Small amount of liquid formed
60	1384°	Liquid + solid
70	1396°	Liquid + solid (color gradation)
70	1402°	Liquid + solid
80	1426°	Liquid + solid (X-ray:PbO+ZrO_2+PZT)
90	1460°	?

away from this area to provide the heat of fusion. This conclusion is borne out by the disappearance of the dip at the second inflection point when the heating rate is lowered.

The last inflection on heating is the liquidus point. After reaching this temperature, the melt temperature rises very rapidly due to heat conduction in the liquid to establish a heating rate similar to that of the furnace. A summary of results is in Table X and Fig. 29.

The heating curves show a trend that would support the idea of a three phase region containing liquid ZrO_2 + PZT does exist at high temperatures. The results agree well with those obtained from quenching techniques as depicted in Fig. 30. The major refinements to the quenching diagram are the lower solidus and liquidus temperatures due to greater sensitivity in detection, the determination of the peritectic temperature to be 1360 rather than 1340°C, and the estimated extension of the peritectic isotherm to approximately 40 mole % $PbZrO_3$.

The establishment of a three phase region in the $PbTiO_3$-$PbZrO_3$ system definitely proves the system is not a quasi binary section in the PbO-TiO_2-ZrO_2 composition temperature diagram.

TABLE X. Summary of heating curve analysis

Composition mole % $PbZrO_3$	Heating rate ° min.	Lower temp. °C	Middle	Upper temp. °C
0	4	1286	--	1289
0	8	1286	--	1289
5	2.5	1289	--	1314
5	6	1282	1300	1312
5	8	1272	1305	1318
10	2.5	1294	1319	1327
10	6	1294	1312	1329
10	8	1294	1315	1334
15	2.5	1291	1322	1355
15	6	1304	1325	--
15	100	1299	1322	1349
20	2.5	1315	1334	1357
20	6	1305	1335	1360
20	8	1309	1338	1359
25	2.5	1317	1341	1357
25	6	1325	1345	1359
25	8	1322	1347	1359
30	2.5	1327	1347	1368
30	6	1322	1355	1372
30	8	1322	1354	--
35	2.5	1337	1353	1374
35	8	1335	1360	1374
40	6	1339	1367	1372
52.5	6	1360	1389	1404
60	6	1375	1408	1431
70	6	1396	1431	1456
80	6	1426	--	1489

IV. SUMMARY AND CONCLUSIONS

Investigations of the $PbTiO_3$-$PbZrO_3$ system were undertaken using X-ray, vapor loss, differential thermal and thermal analysis.

Lead zirconate titanate formed by mixing PbO, TiO_2, and ZrO_2 powders and calcining at 800°C were shown to be inhomogeneous. Homogenization could be achieved by a high temperature heat treatment.

A solid solution is shown to exist in the region between the Curie and solidus temperatures. X-ray, differential thermal and thermal analyses failed to detect any phase transition in this region. Experiments in the solid solution region conducted in vacuum at 1050°C and 1100°C show that vaporization of lead oxide results in compositional changes at the sample's surface. As a consequence of the lead oxide depletion layer one or more new phases are detected by X-ray analysis. These were identified as ZrO_2, TiO_2, and $ZrTiO_4$.

The congruent melting point of $PbTiO_3$ was determined to be 1286 ± 3°C by thermal analysis. Similar experiments with $PbZrO_3$ were unsuccessful because the sample rapidly attacked the crucible above 1500°C.

The final temperatures used for the phase diagram were obtained from heating curve analysis. Cooling curves proved to be inaccurate due to supercooling and segregation in the final solid. Not only are the temperatures obtained by heating curves more reliable than those obtained from cooling curves, but the problem of nucleation and growth of nonequilibrium phases is not present. The solidus temperature has been determined to increase with increased lead zirconate to leat titanate ratio. At 1360°C a peritectic reaction occurs for compositions between 15 to approximately 40 mole % $PbZrO_3$. Above the peritectic

temperature is a three phase region with liquid, zirconia and lead zirconate titanate solid solutions in equilibrium. Compositions richer in $PbZrO_3$ than 40 mole % decompose directly to three phases at the solidus temperature. Compositions between $PbTiO_3$ and 15 mole % $PbZrO_3$ show a simple melting behavior characteristic of a solid solution.

The phase diagrams determined by heating curve and quenching analyses are in basic agreement. Temperatures obtained from heating curve methods are believed to be the most accurate because phase transitions can be detected with greater sensitivity.

As a result of the decomposition reaction, the $PbZrO_3$-$PbTiO_3$ phase diagram cannot be considered a true binary system, but simply a vertical section in the PbO-TiO_2-ZrO_2 composition-temperature diagram.

ACKNOWLEDGEMENTS

The writer wishes to thank Prof. R. M. Fulrath for his guidance during this investigation. The author also should like to thank R. Gioque for chemical analysis, G. Pelatowski for figure reproduction, M. Stett for periodic references, K. Radmilovic, P. Cookson, C. Machen, S. Sparks for typing, A. Bugaeff, W. O'Neil, J. Wodei, L. Seaborn, T. Somerville and J. Frease for experimental assistance. A great deal of appreciation is expressed to my fellow graduate students for their valuable comments and to my wife Cecile for her help and encouragement.

This work was done under the auspices of the United States Atomic Energy Commission.

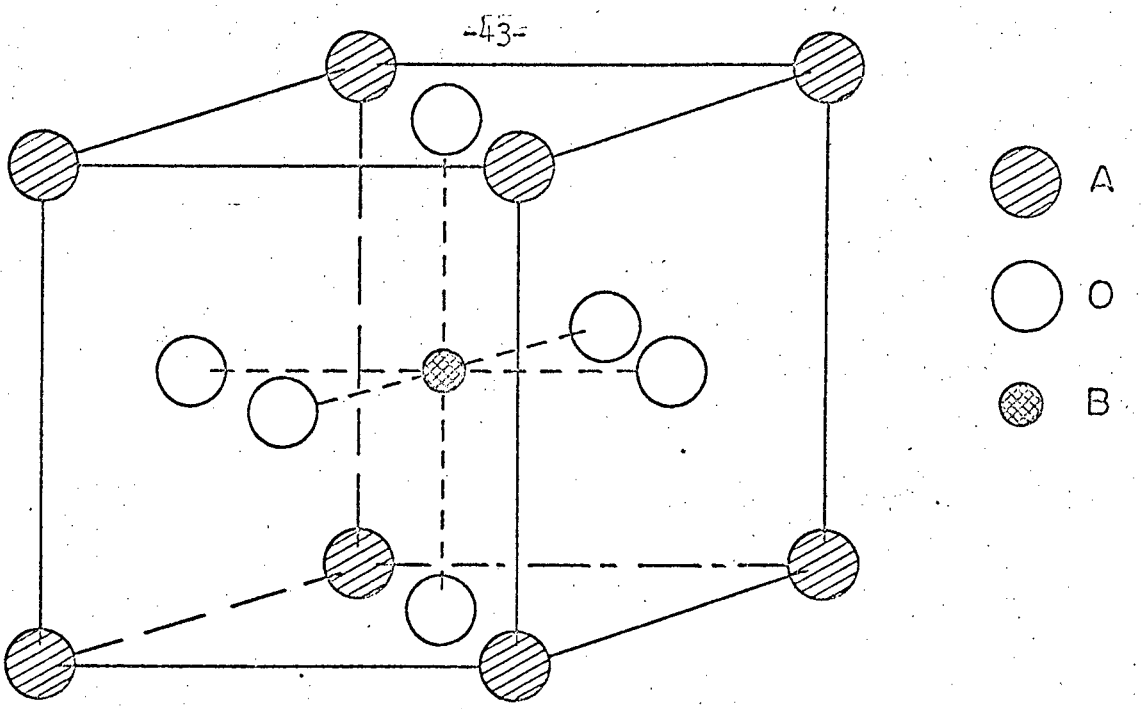

Cubic perovskite structure.

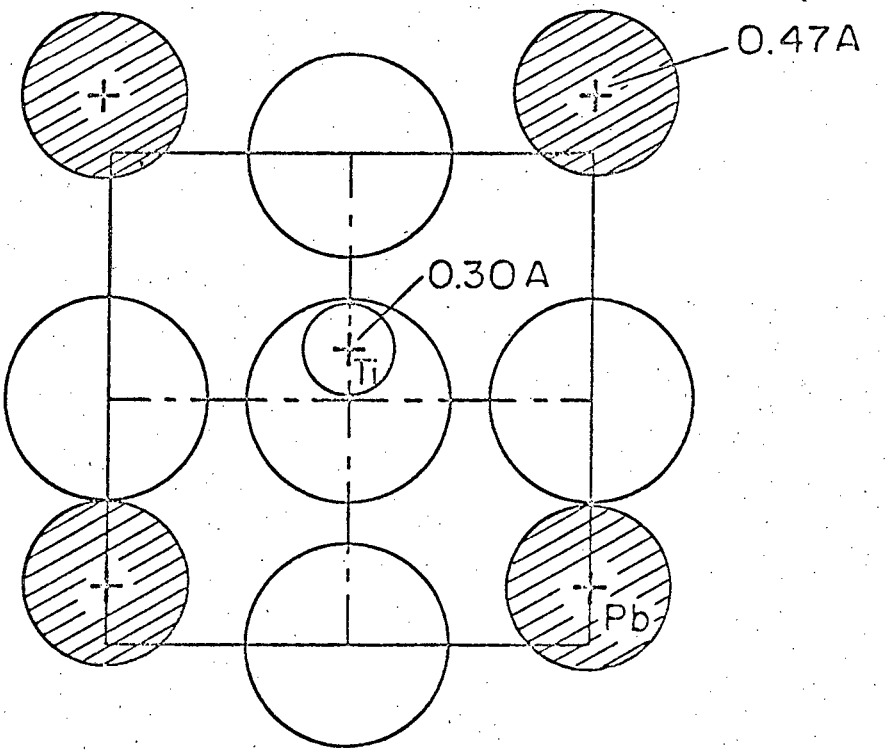

Schematic model of the structure for $PbTiO_3$ at room temperature showing shift of Pb and Ti ions relative to the oxygen octahedron.

Fig. 1 High and low temperature structures of $PbTiO_3$.[8]

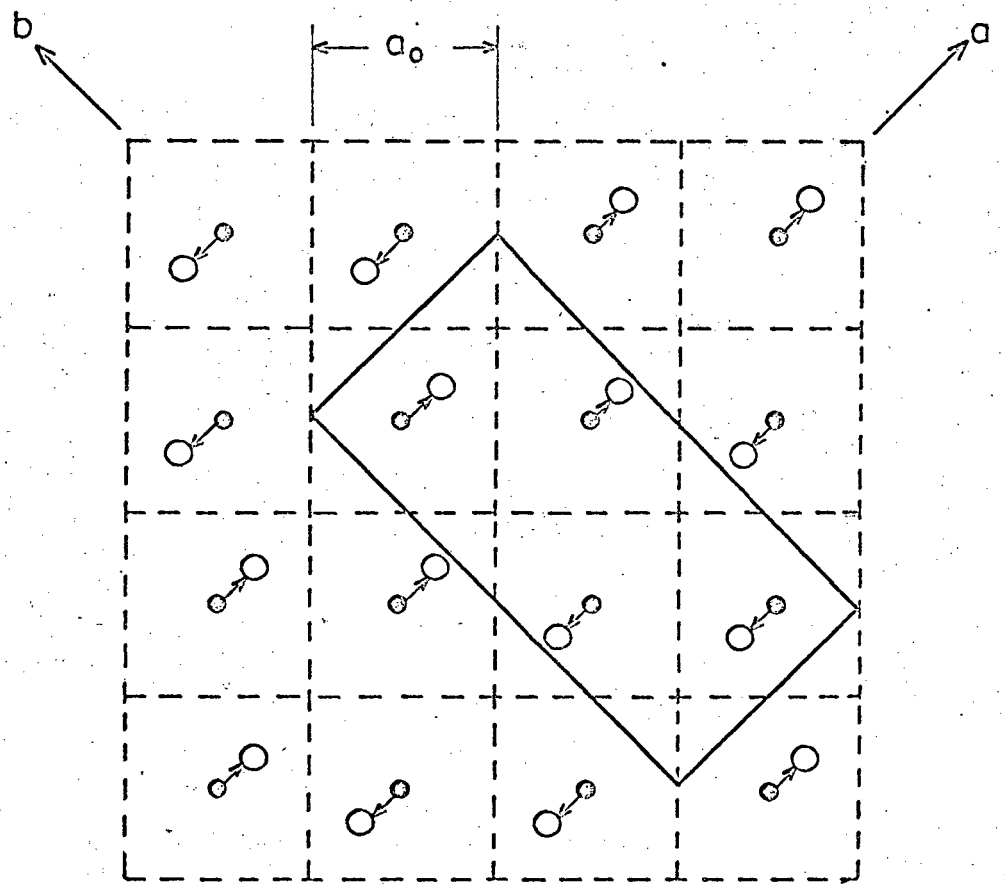

Schematic projection on (001) of the antiferroelectric structure of $PbZrO_3$.

Fig. 2 Antiferroelectric structure of $PbZrO_3$

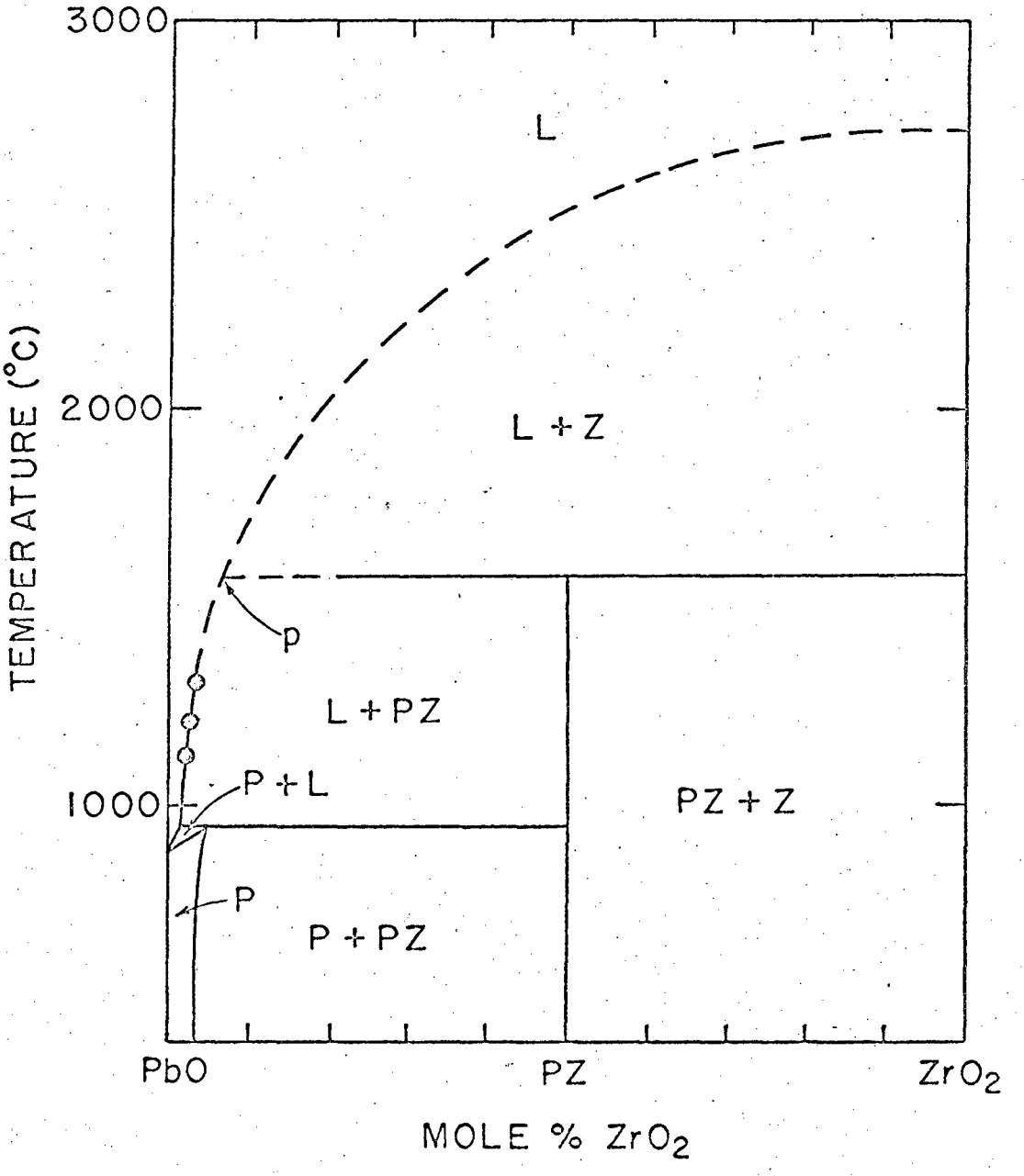

Fig. 3 Phase diagram of PbO-ZrO_2 system[26]

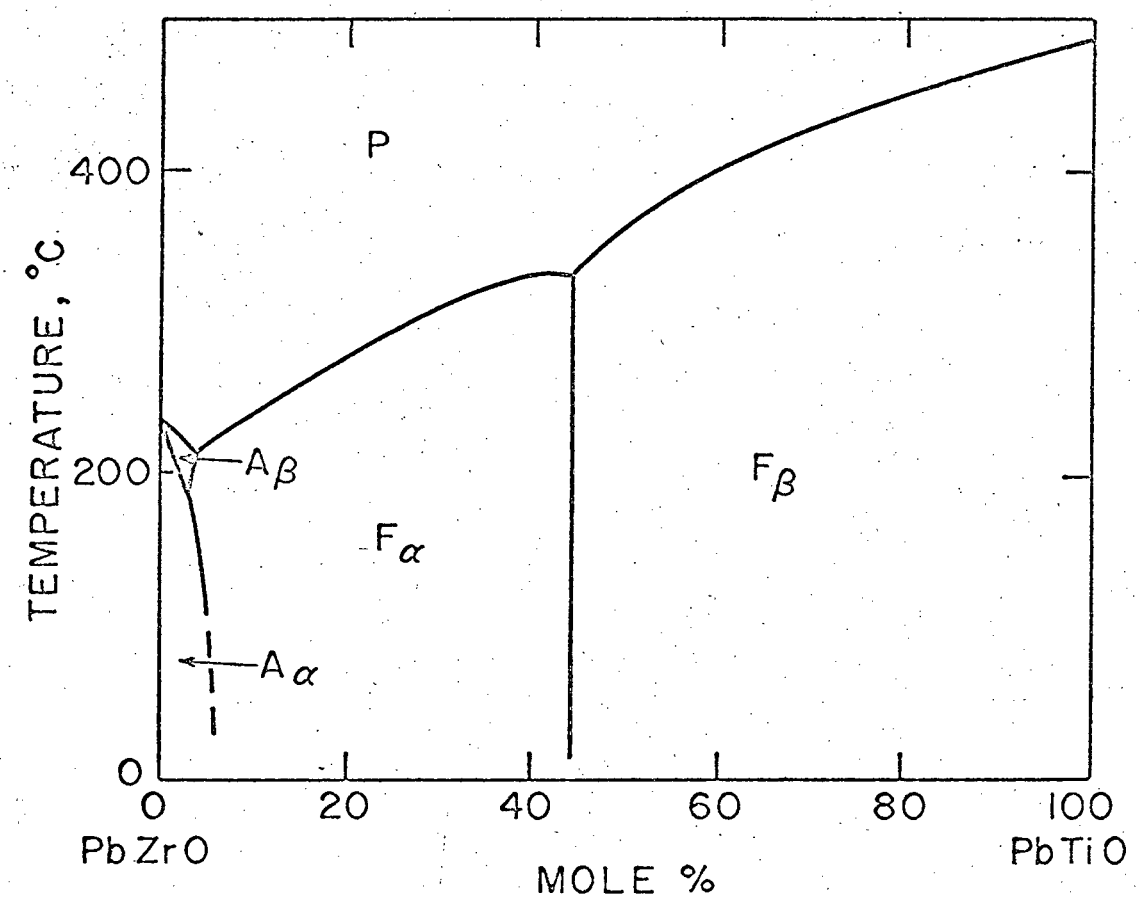

P = Paraelectric, cubic phase

A_α = Antiferroelectric, orthorhombic phase

A_β = Antiferroelectric

F_α = Ferroelectric, rhombohedral phase

F_β = Ferroelectric, tetragonal phase

E. Sawaguchi, J. Phy. Soc. Japan
8, 615 (1953)

Fig. 4 Low temperature phase diagram of $PbTiO_3$-$PbZrO_3$ system

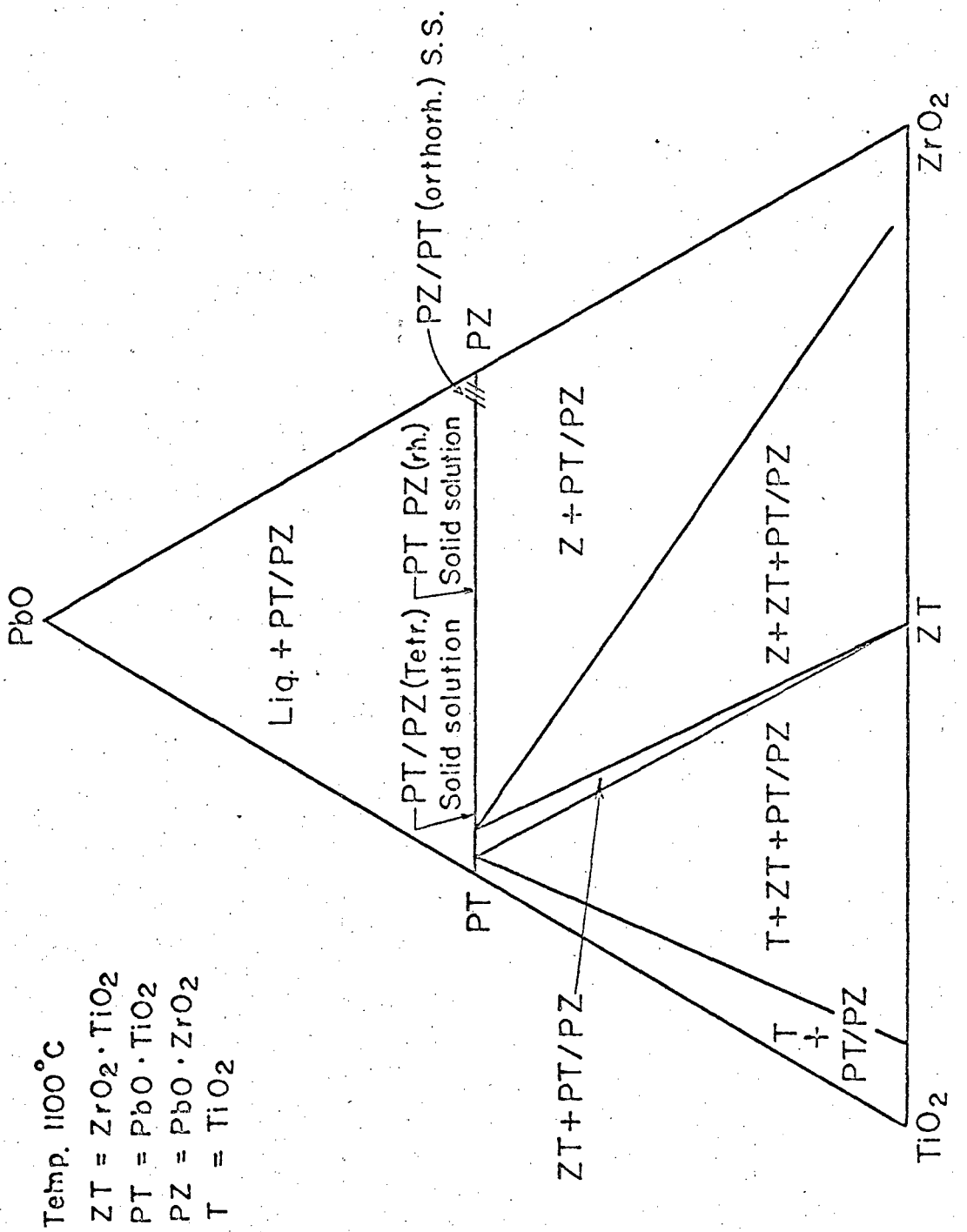

Fig. 5 Reaction diagram of the PbO-TiO_2-ZrO_2 system at 1100°C[16,35]

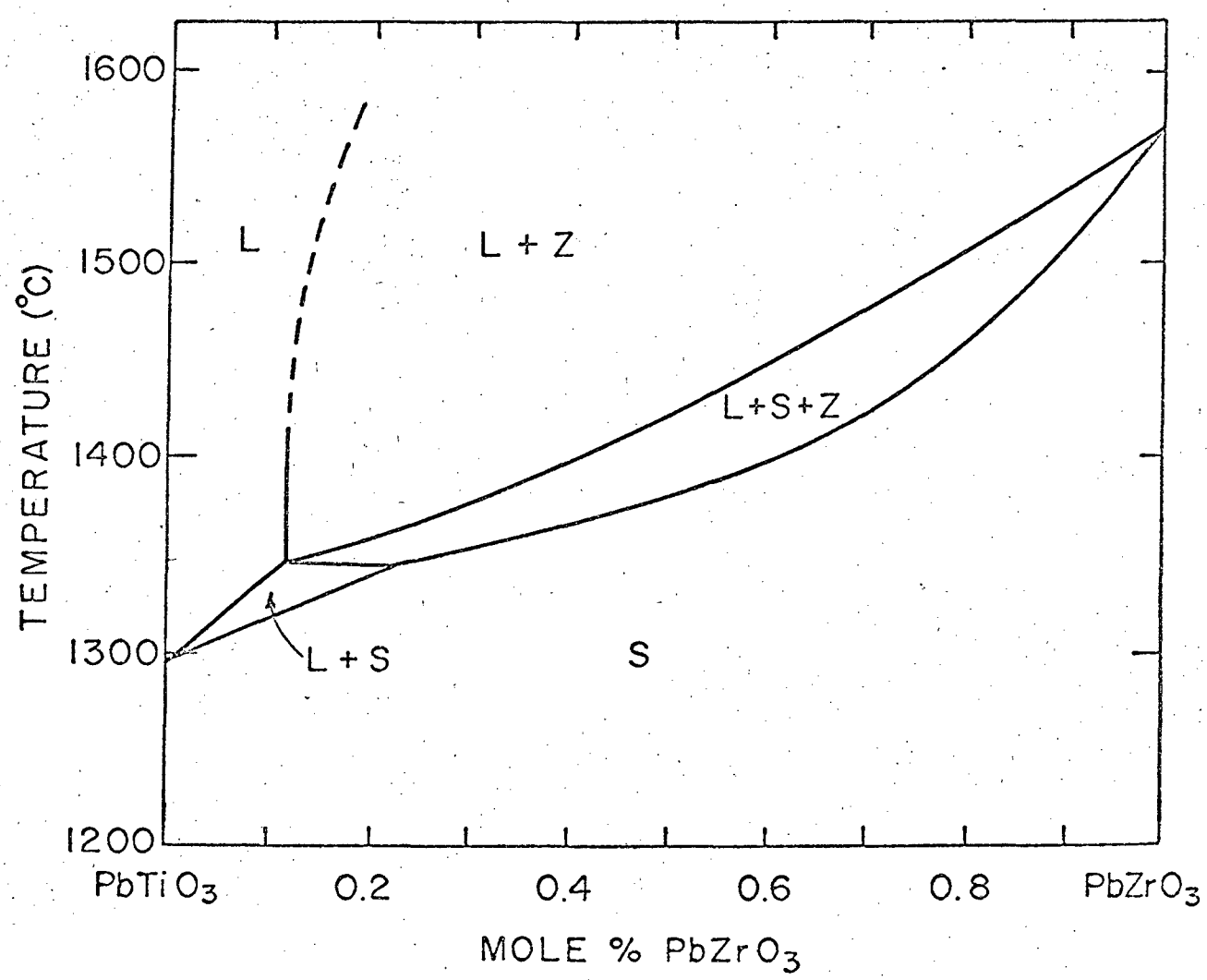

L = LIQUID

Z = ZrO_2 RICH SOLID

S = LEAD ZIRCONATE TITANATE

Fig. 6 High temperature composition-temperature diagram of the $PbTiO_3$-$PbZrO_3$.[26]

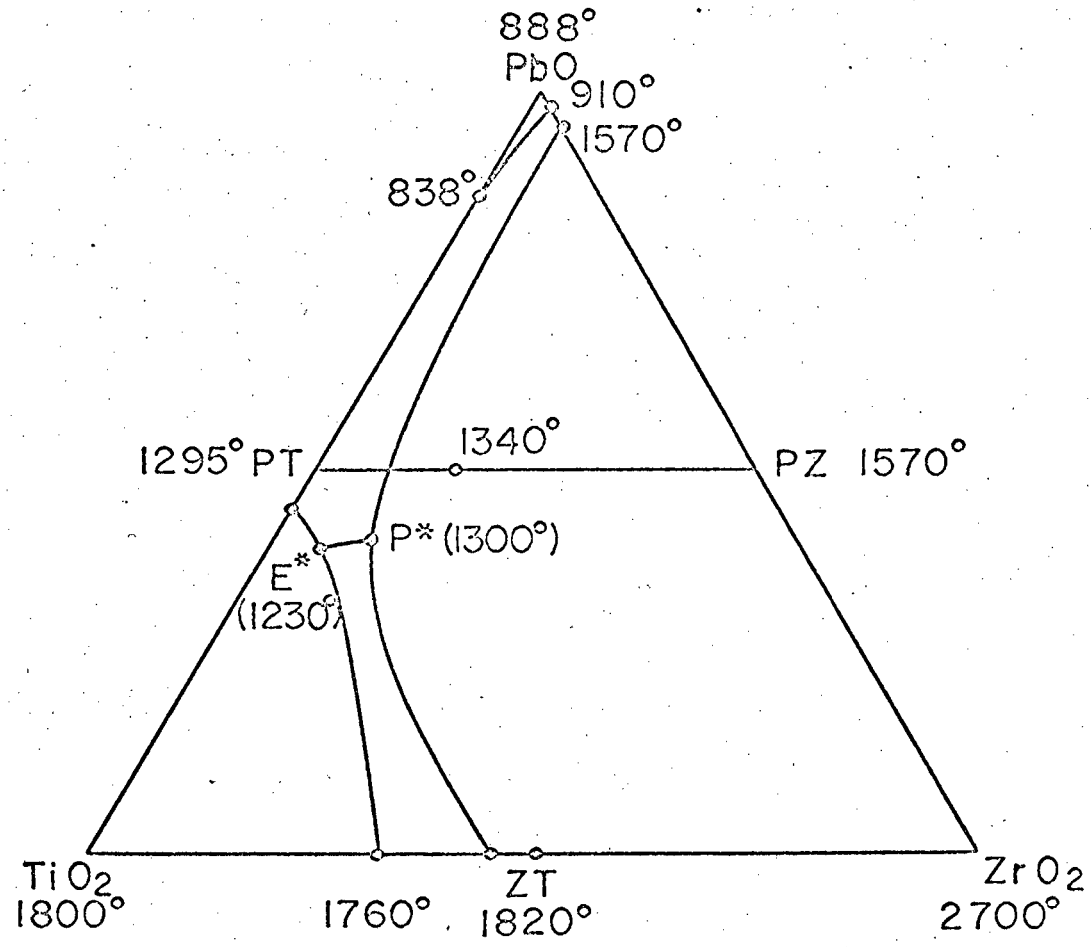

E* TERNARY EUTECTIC
P* TERNARY PERITETIC

Fig. 7 Proposed polythermal projection for the PbO-TiO_2-ZrO_2 system.[26]

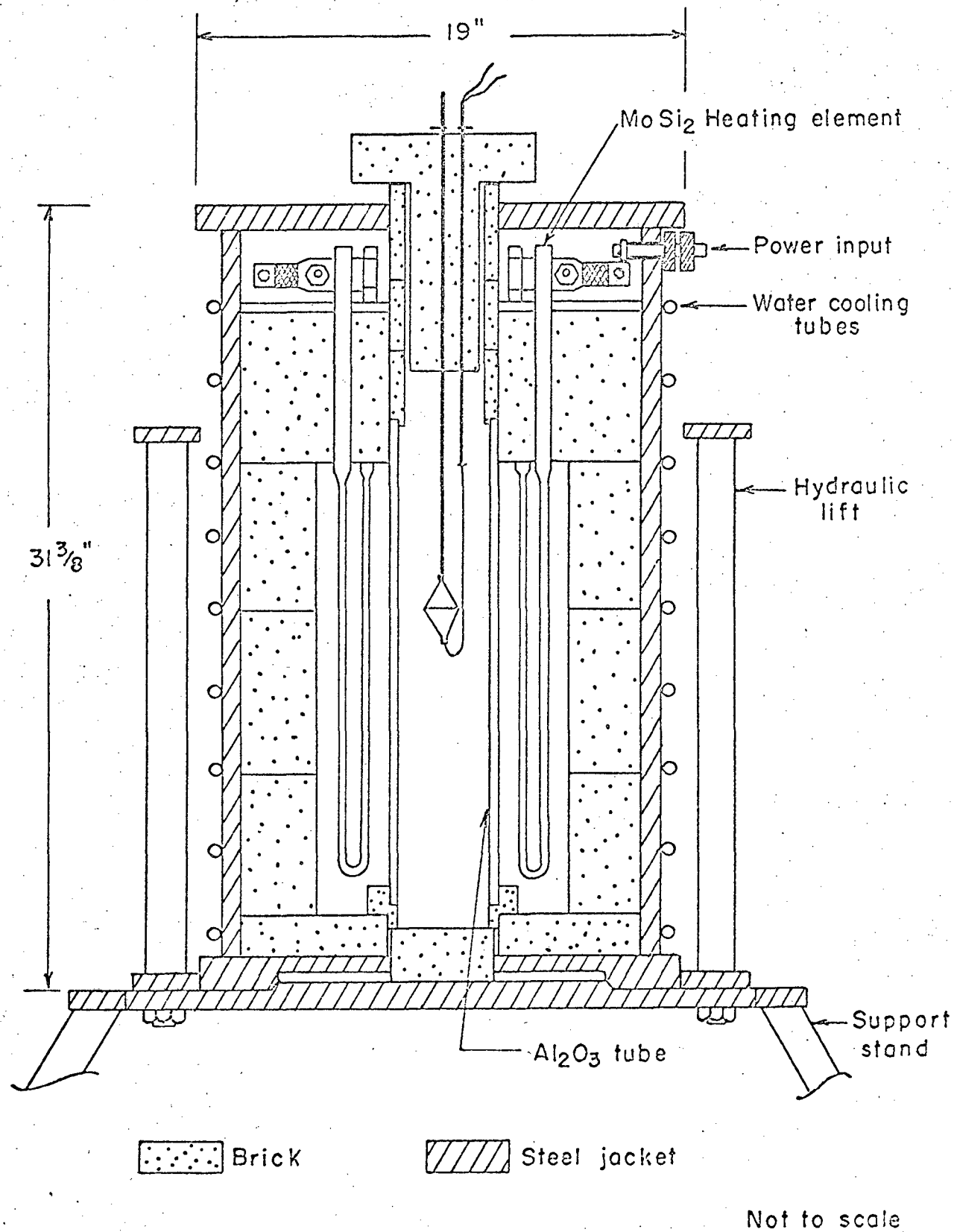

Fig. 8 Furnace for thermal analysis

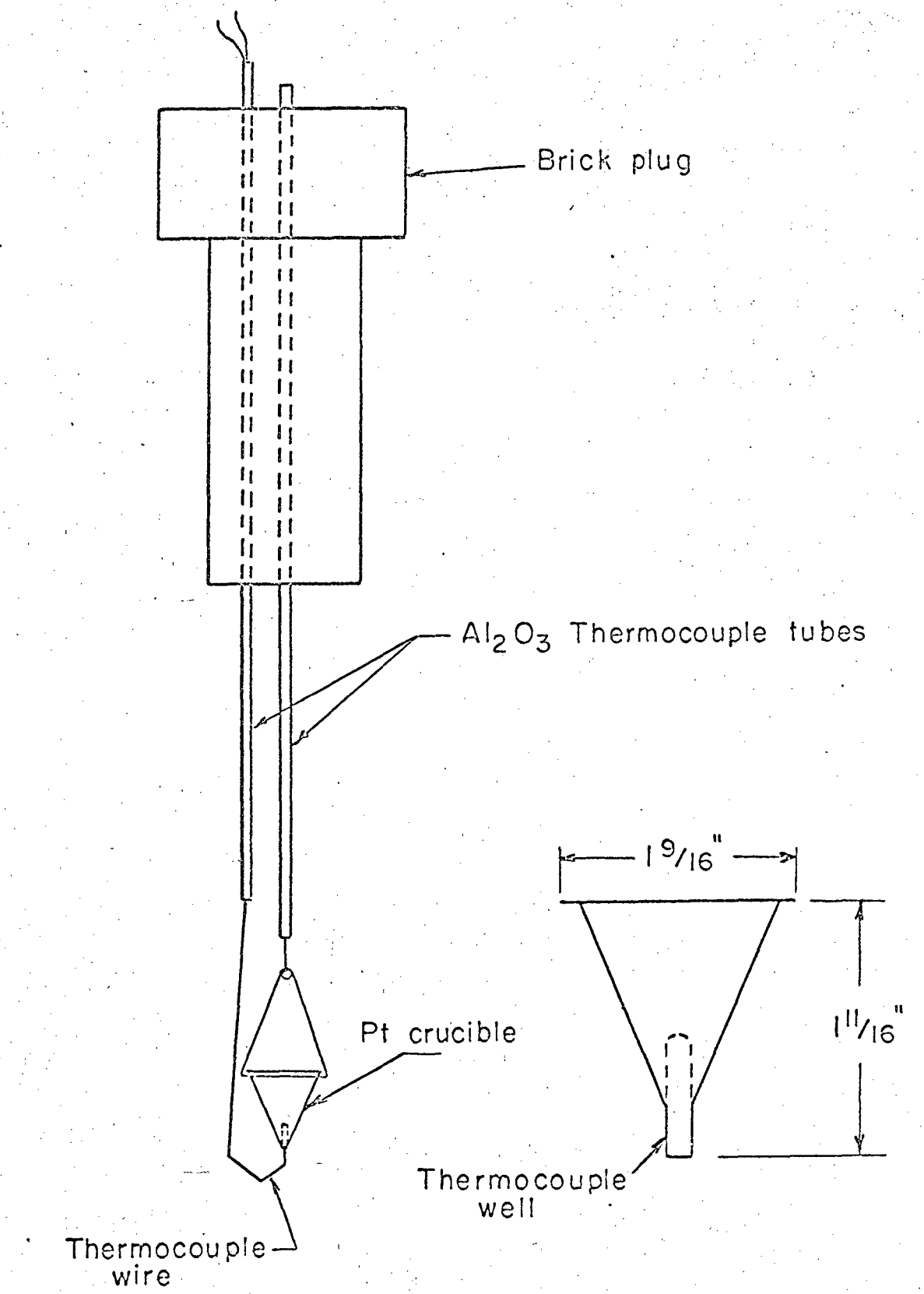

Fig. 9 Suspension apparatus and crucible used for thermal analysis

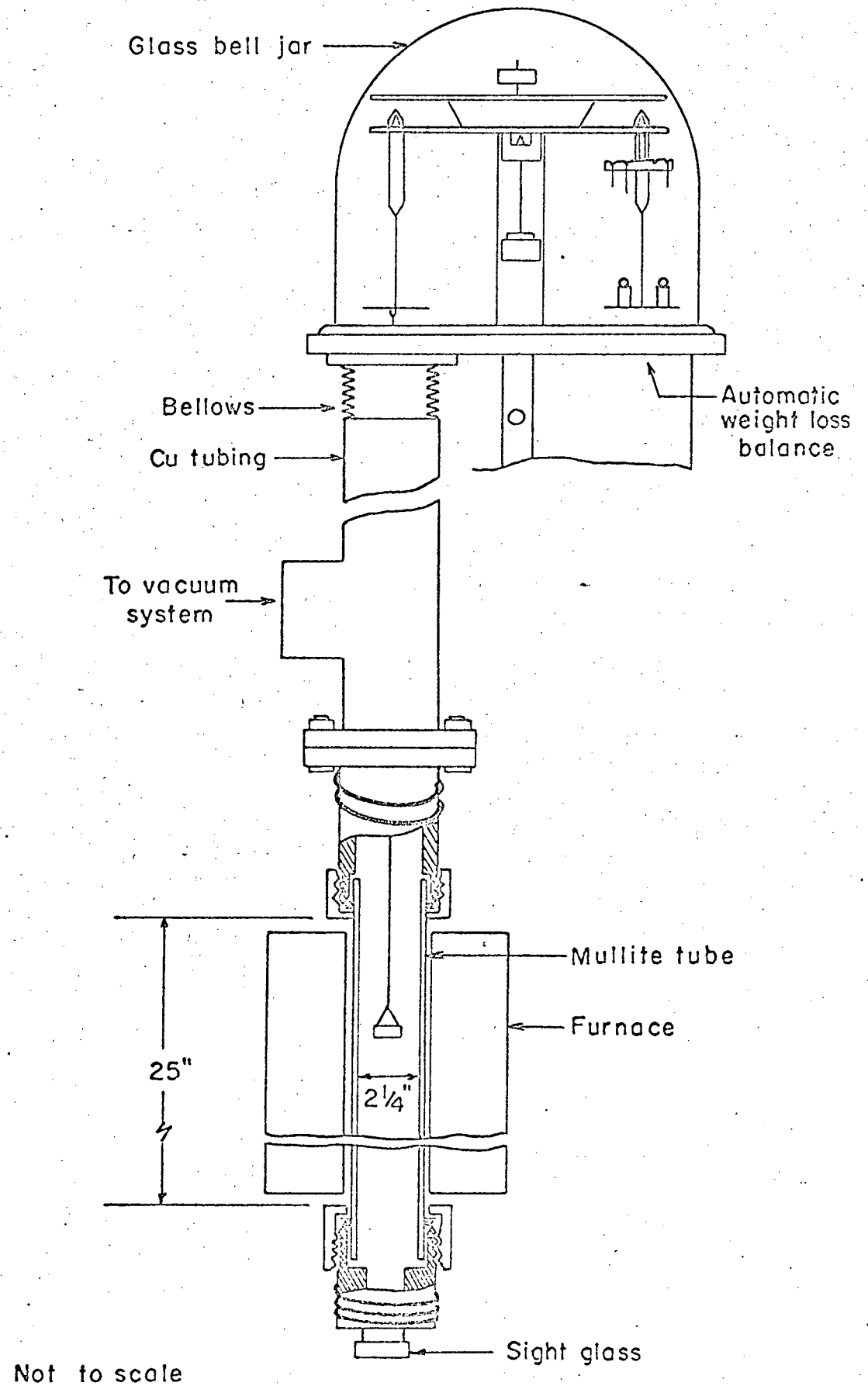

Fig. 10 Weight loss apparatus

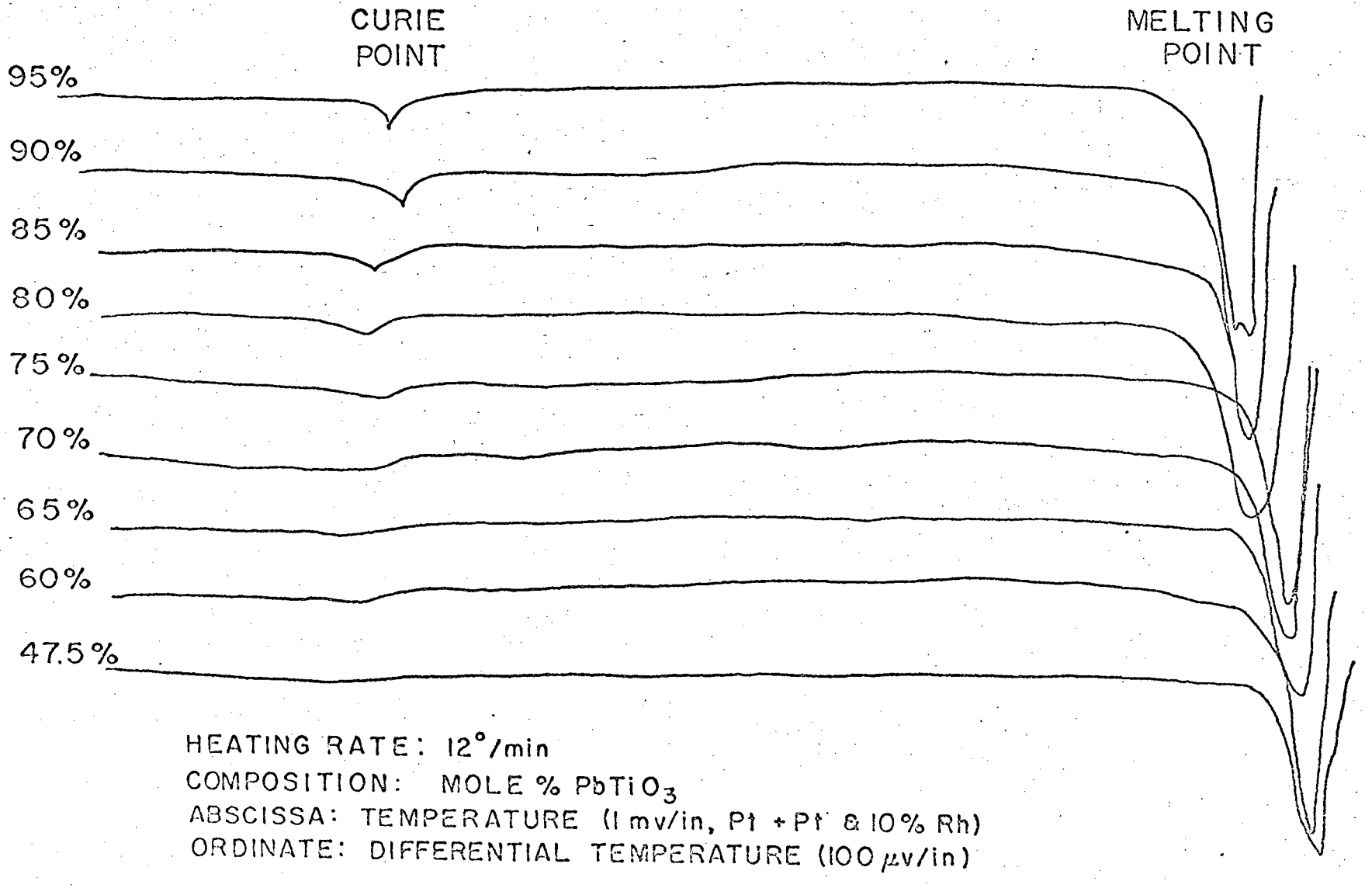

Fig. 11 DTA curves for lead zirconium titanate powders

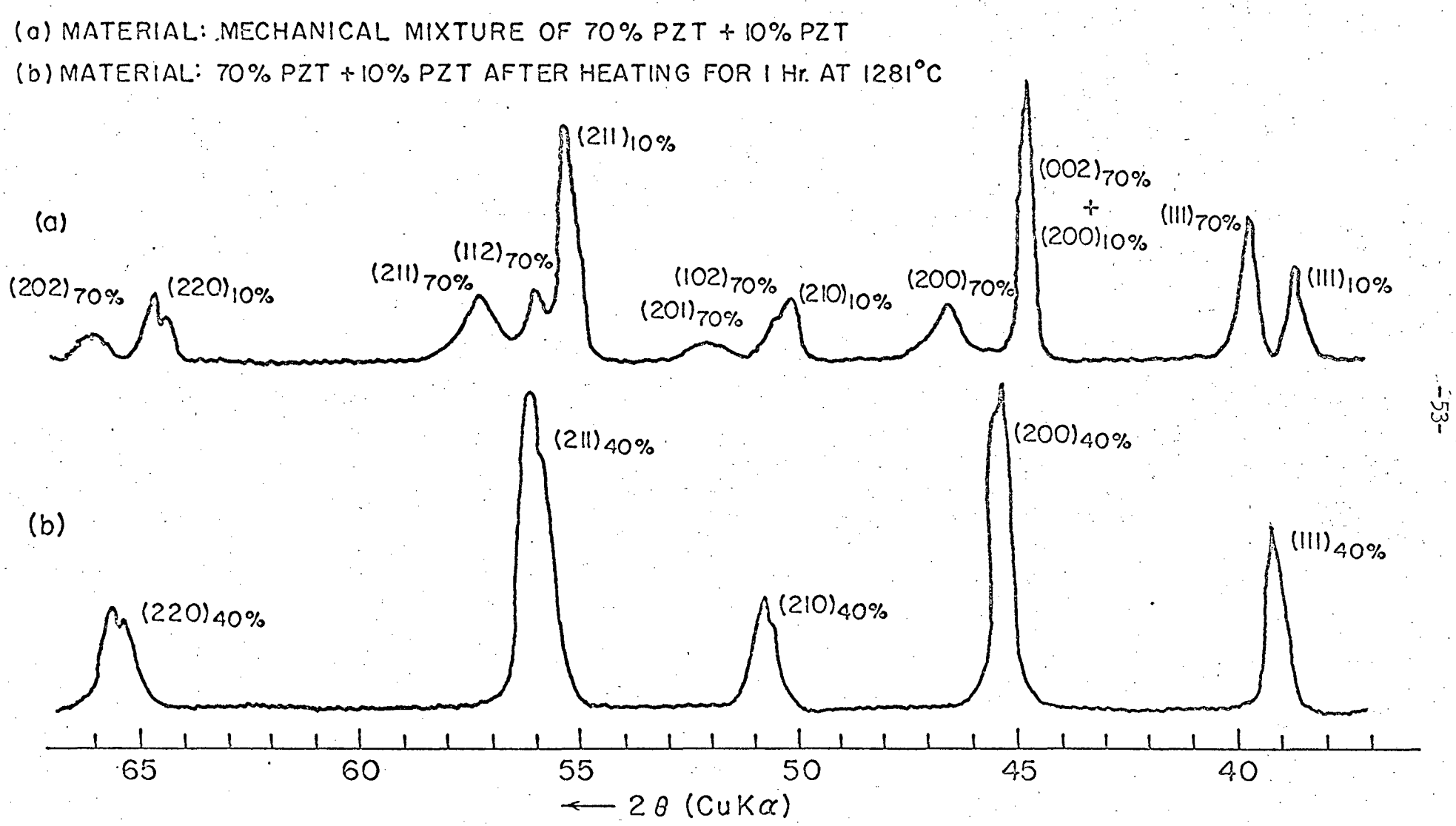

Fig. 12 Typical diffractometer pattern used to determine the existence of a high temperature phase

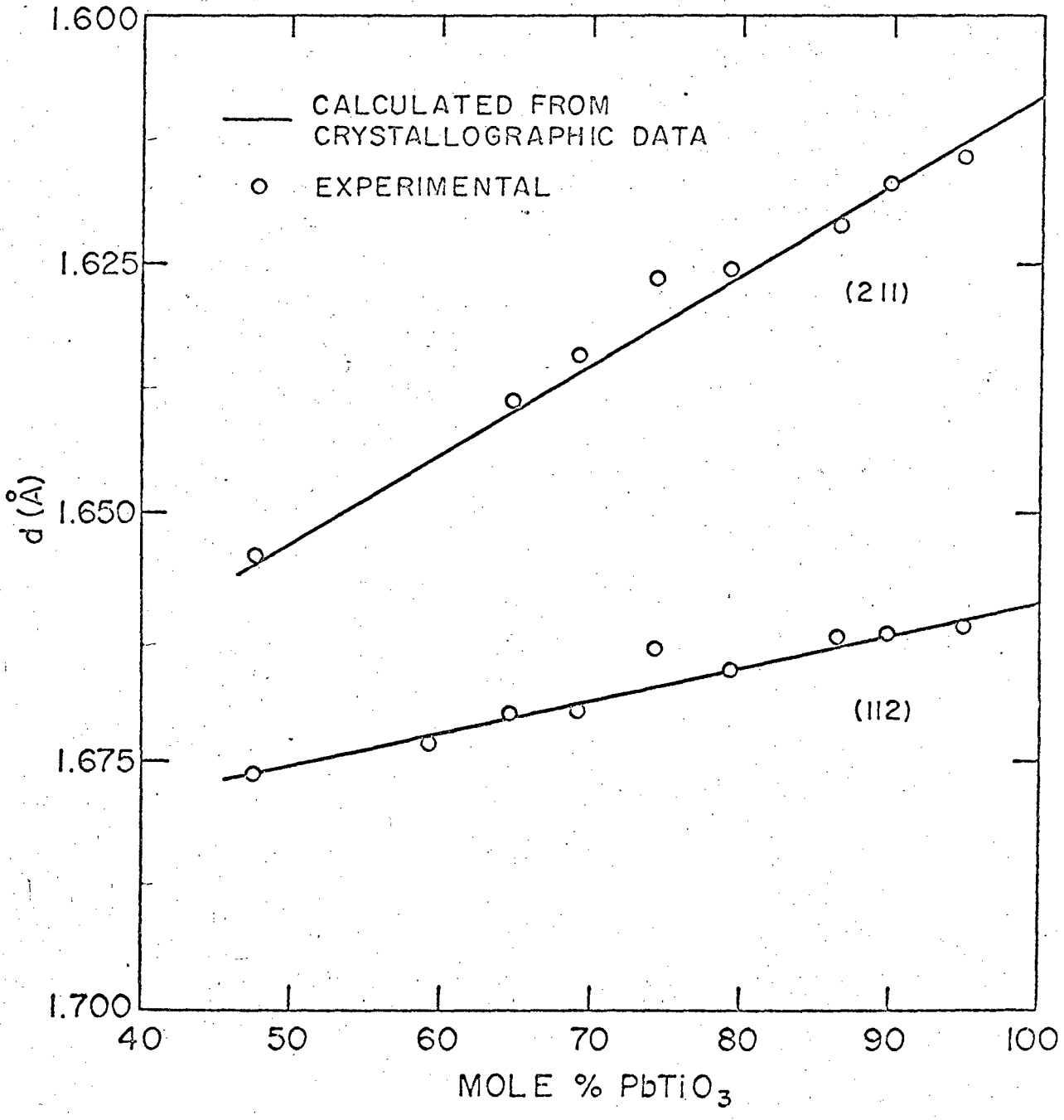

Fig. 13 Interplanar spacings for the (211) and (112) planes of tetragonal PZT

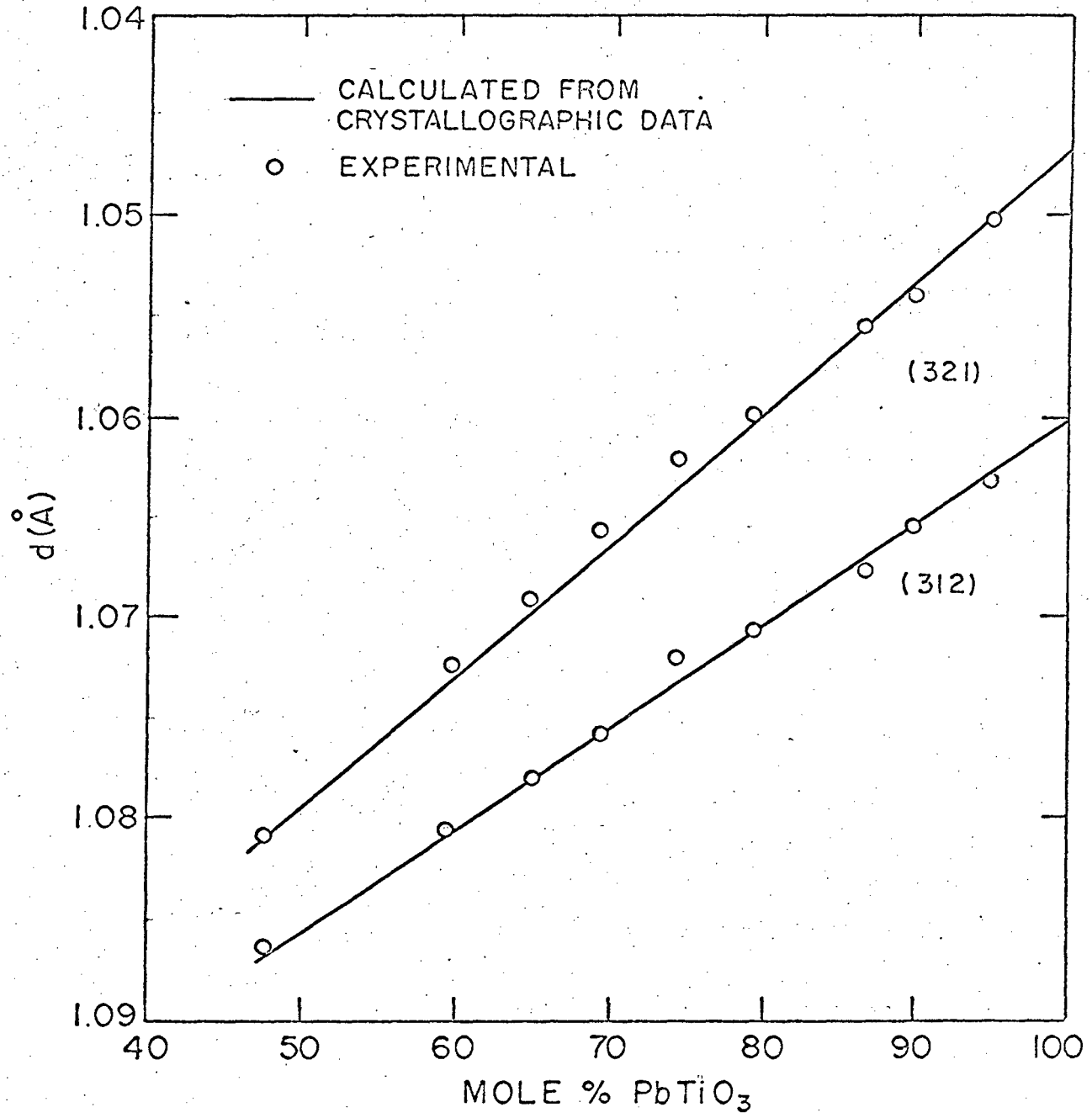

Fig. 14 Interplanar spacings of the (321) and (312) planes for tetragonal PZT

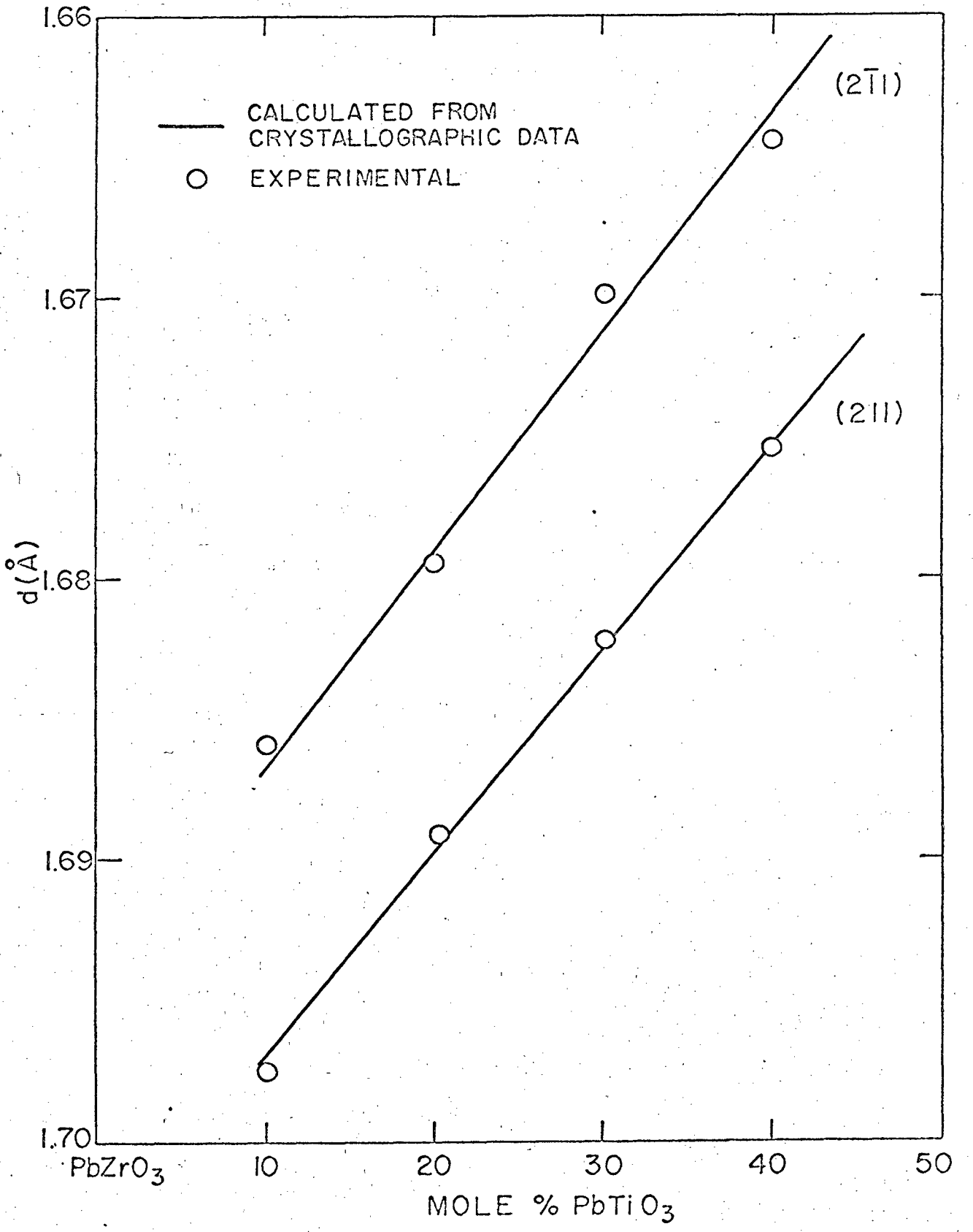

Fig. 15 Interplanar spacings of the (2$\bar{1}$1) and (211) planes for rhombohedral PZT

Composition: $Pb(Zr_{0.20}, Ti_{0.80})O_3$

Radiation: $CuK\alpha$

(a) Calcined powder.

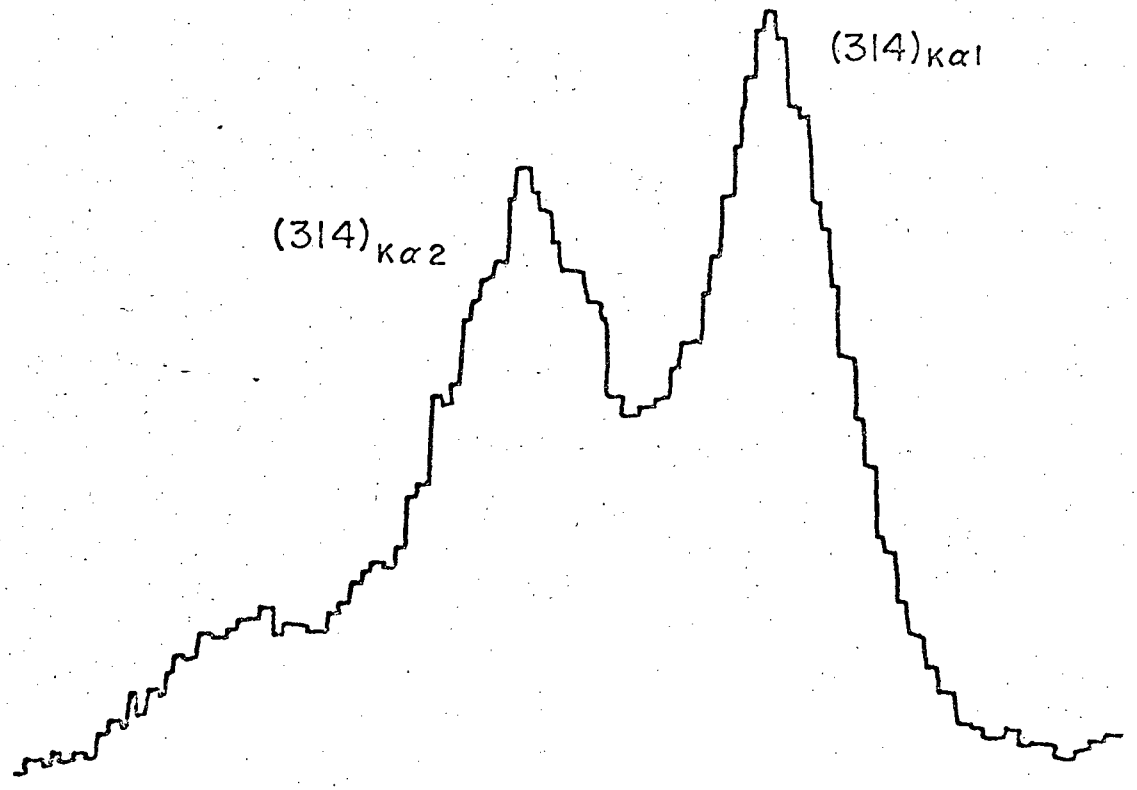

(b) After heating the calcined powder at 1200°C for 1½ hrs.

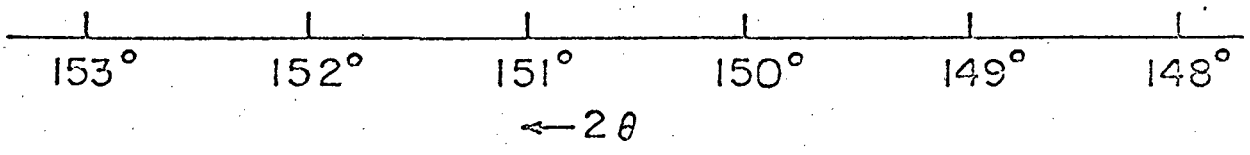

Fig. 16 Diffractometer pattern of (314) peak of $Pb(Zr_{0.20}, Ti_{0.80})O_3$ illustrating the inhomogeneity of calcined powders

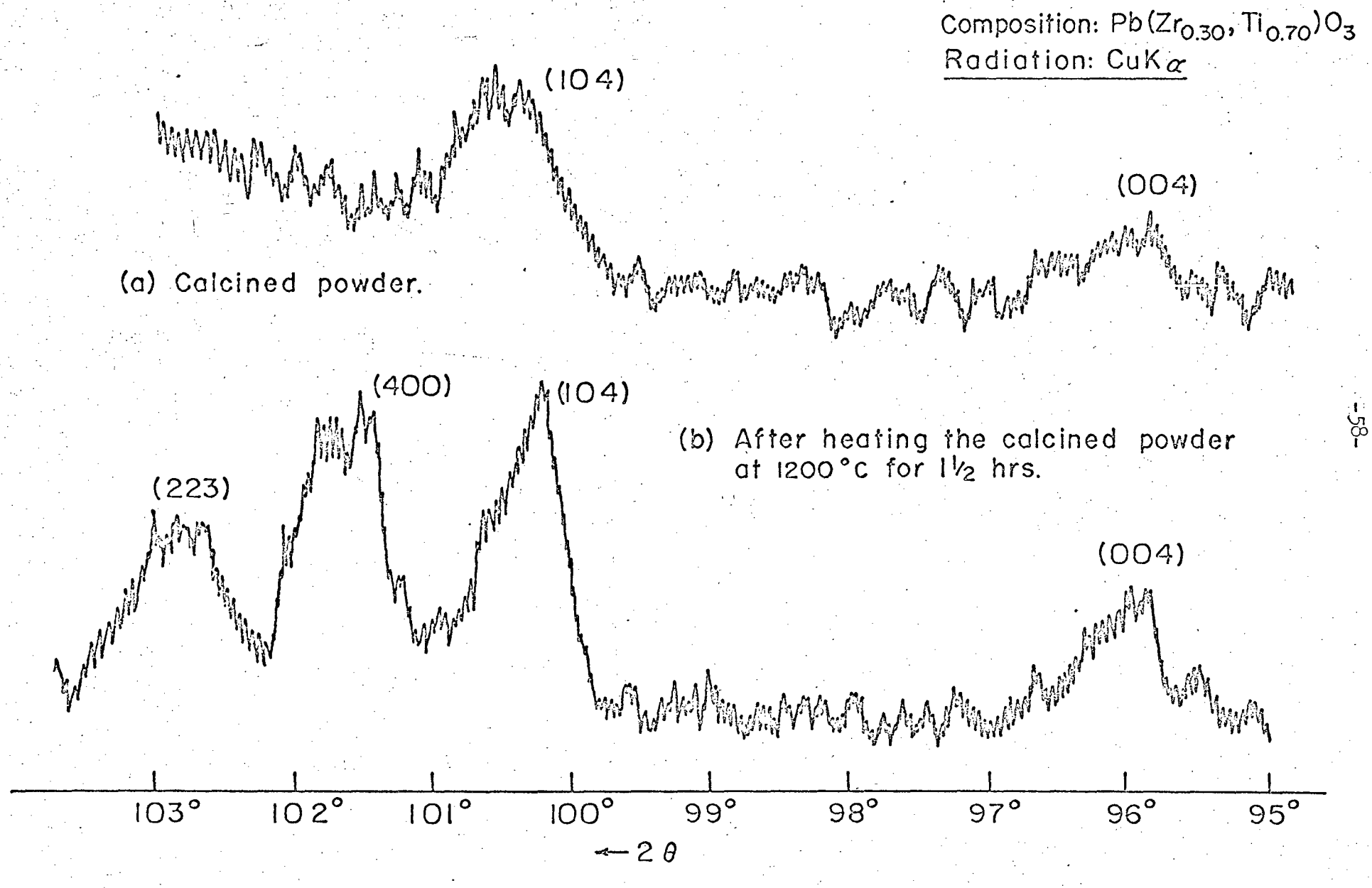

Fig. 17 Diffractometer patterns of (004), (104), (400), (223) peaks of $Pb(Zr_{0.30},Ti_{0.70})O_3$ illustrating the inhomogeneity of calcined powders

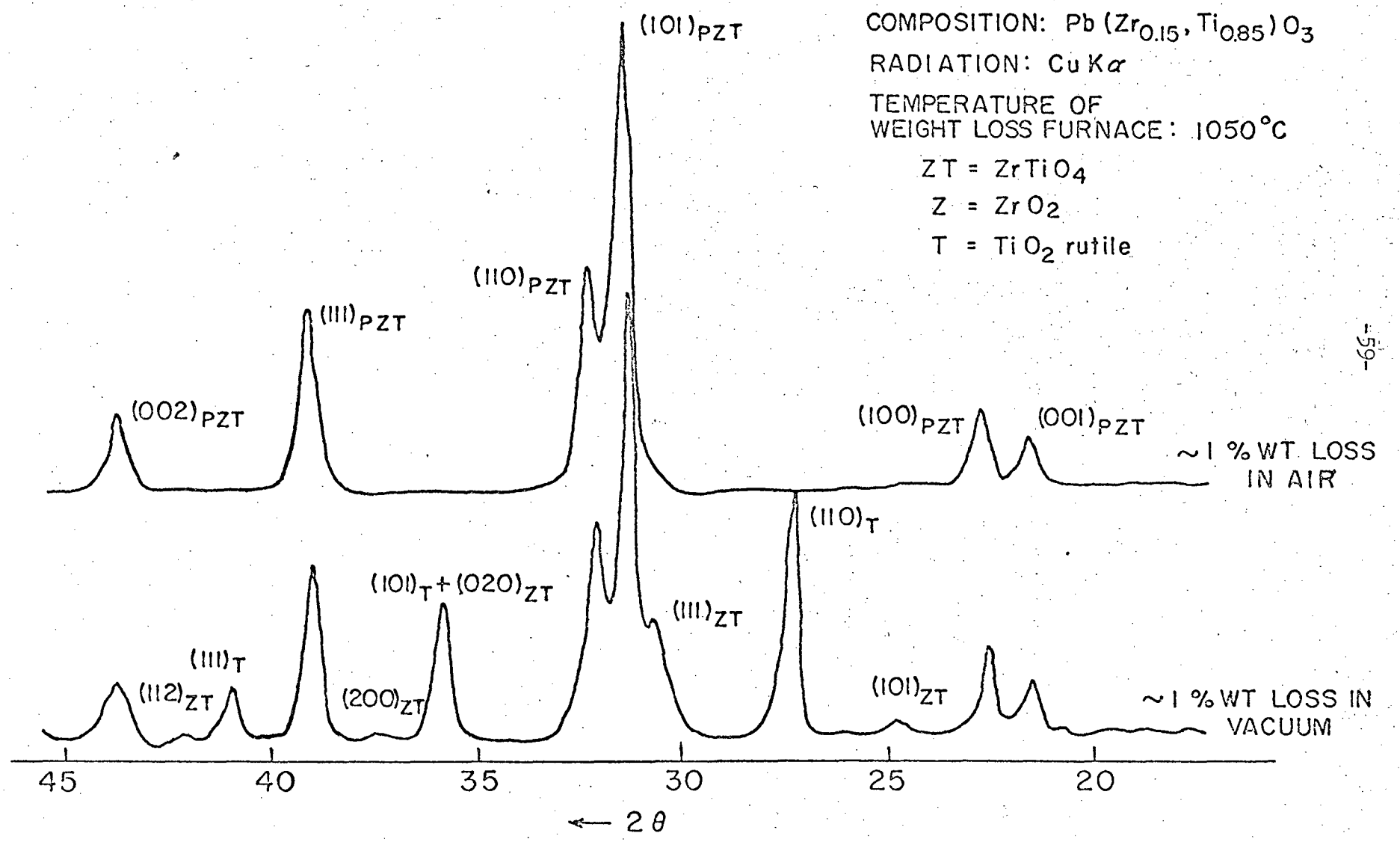

Fig. 18 Comparison of x-ray diffractometer patterns between samples which lost weight in air and in vacuum

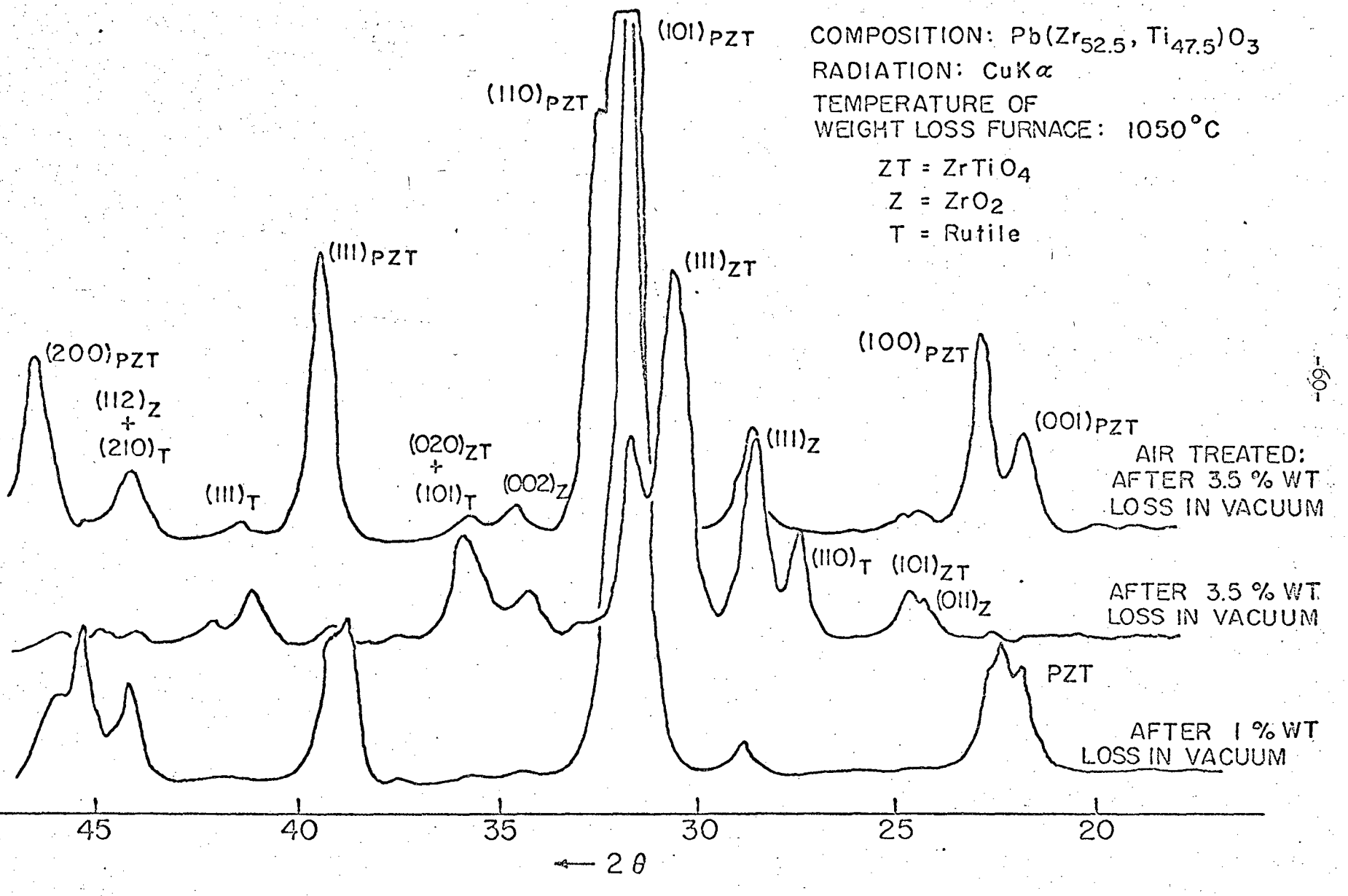

Fig. 19 x-ray patterns showing effect of air treatment to a sample previously in vacuum

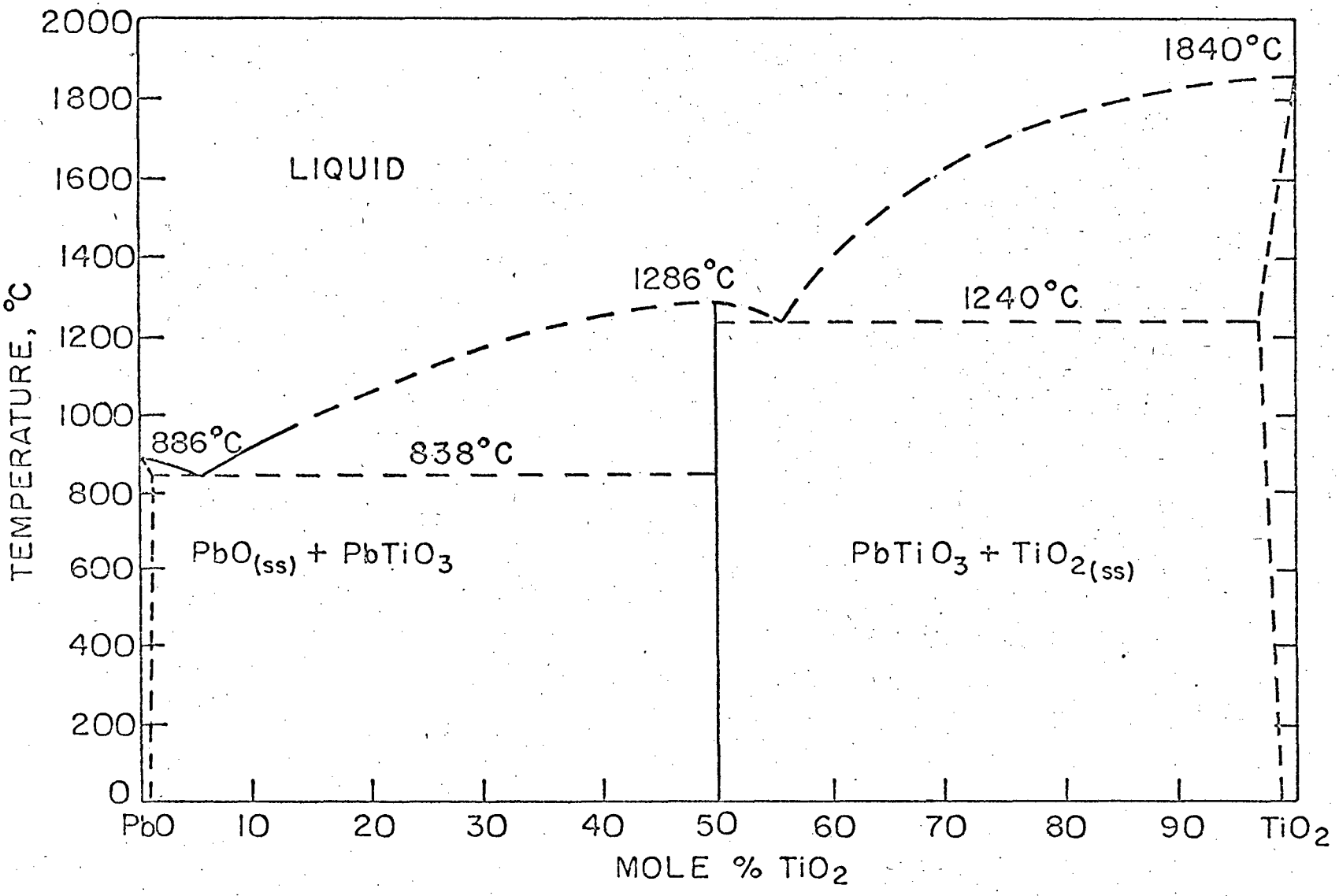

Fig. 20 Proposed phase diagram for $PbO-TiO_2$

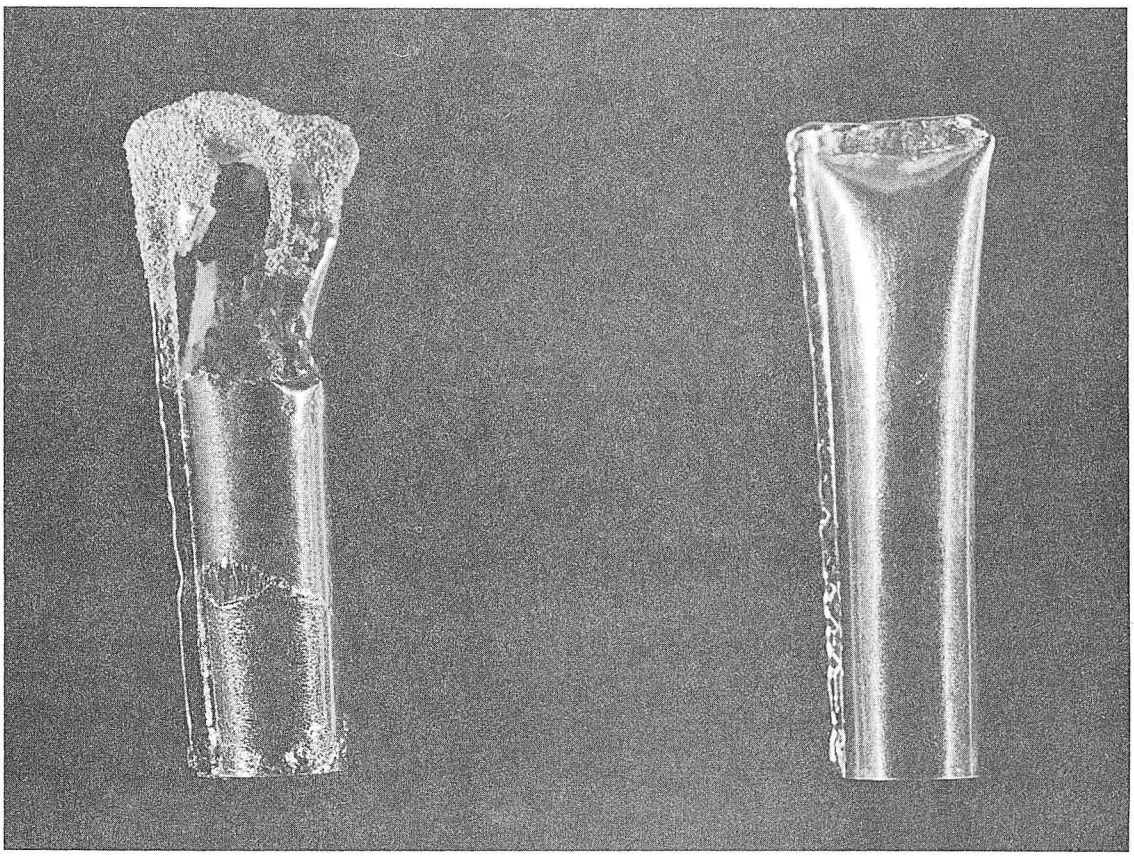

XBB 674-2062

Fig. 21. Comparison of a Pt crucible containing $PbZrO_3$ which was heated to 1520°C compared to an unheated crucible.

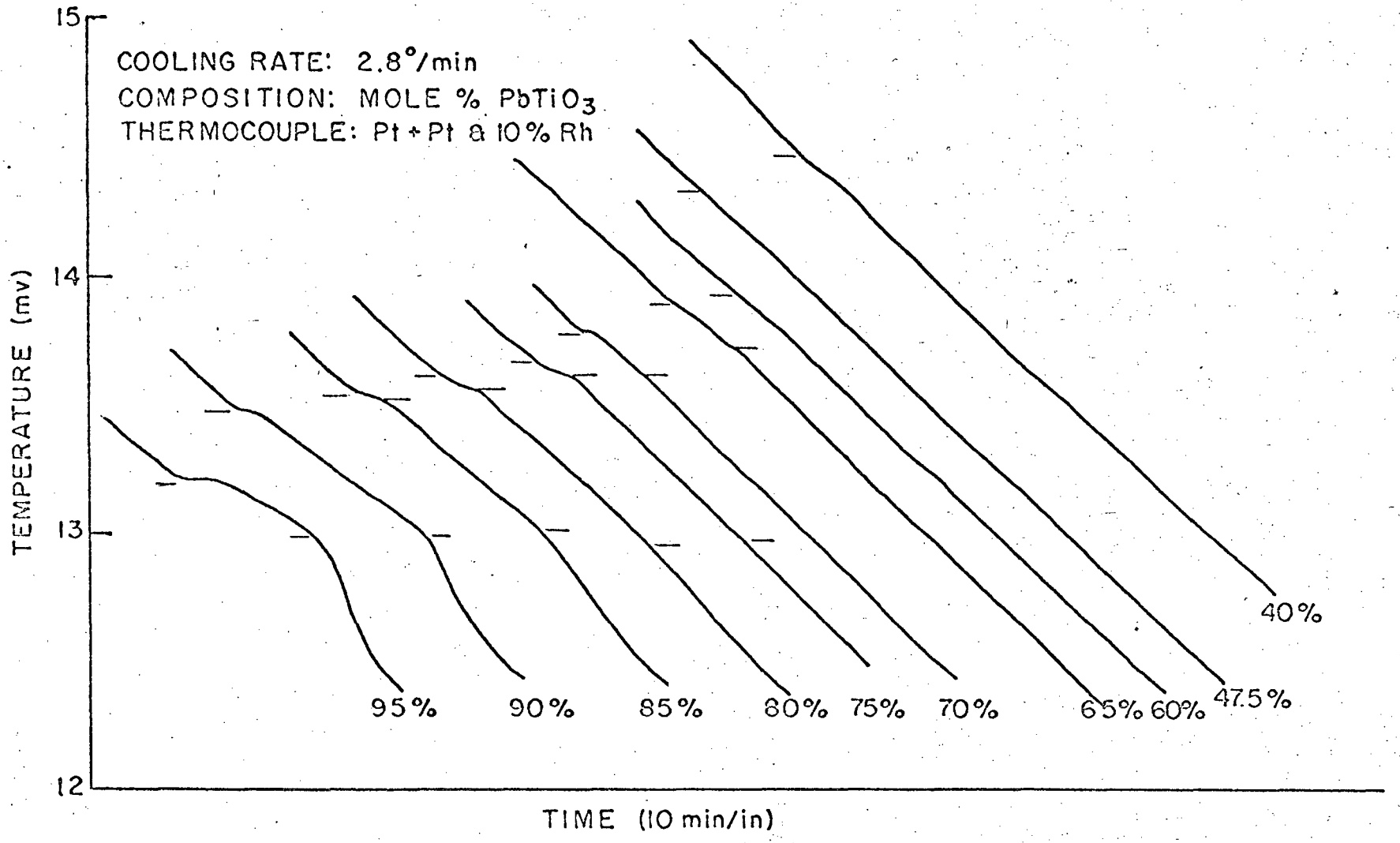

Fig. 22 Cooling curves for a cooling rate of 5.6°/min

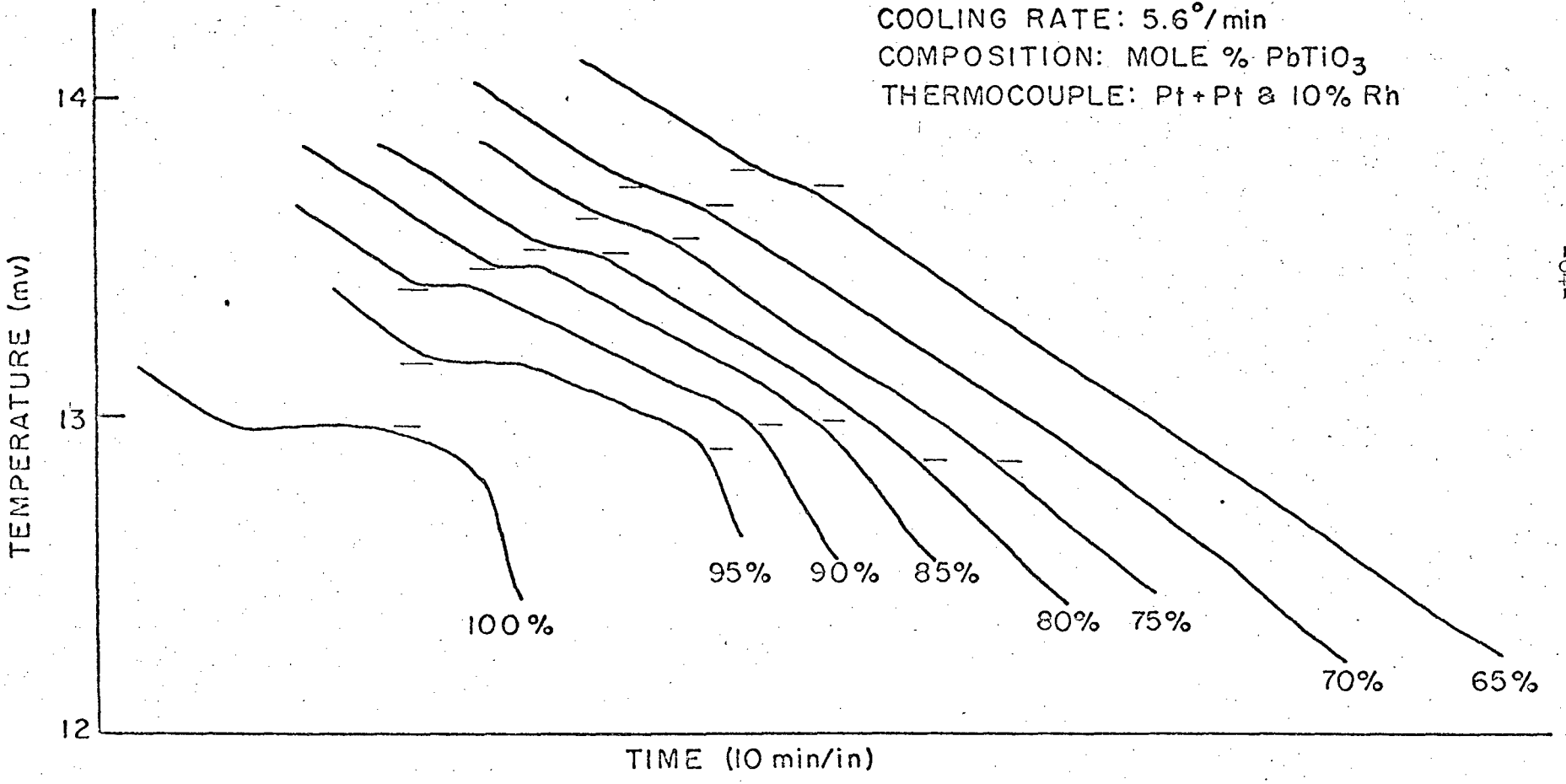

Fig. 23 Cooling curves for a rate of cooling of 5.6°/min

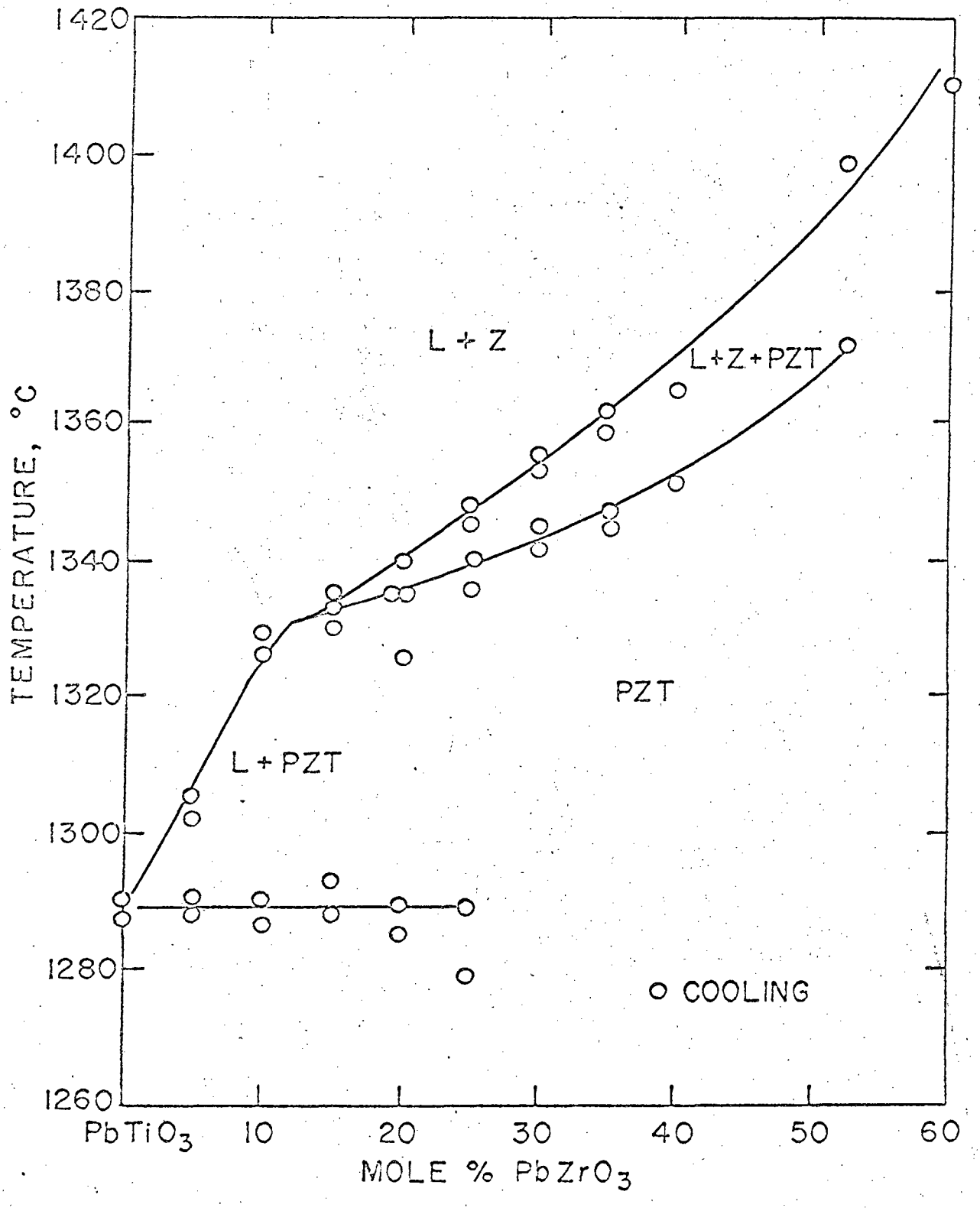

Fig. 24 Phase diagram determined by cooling curve analysis

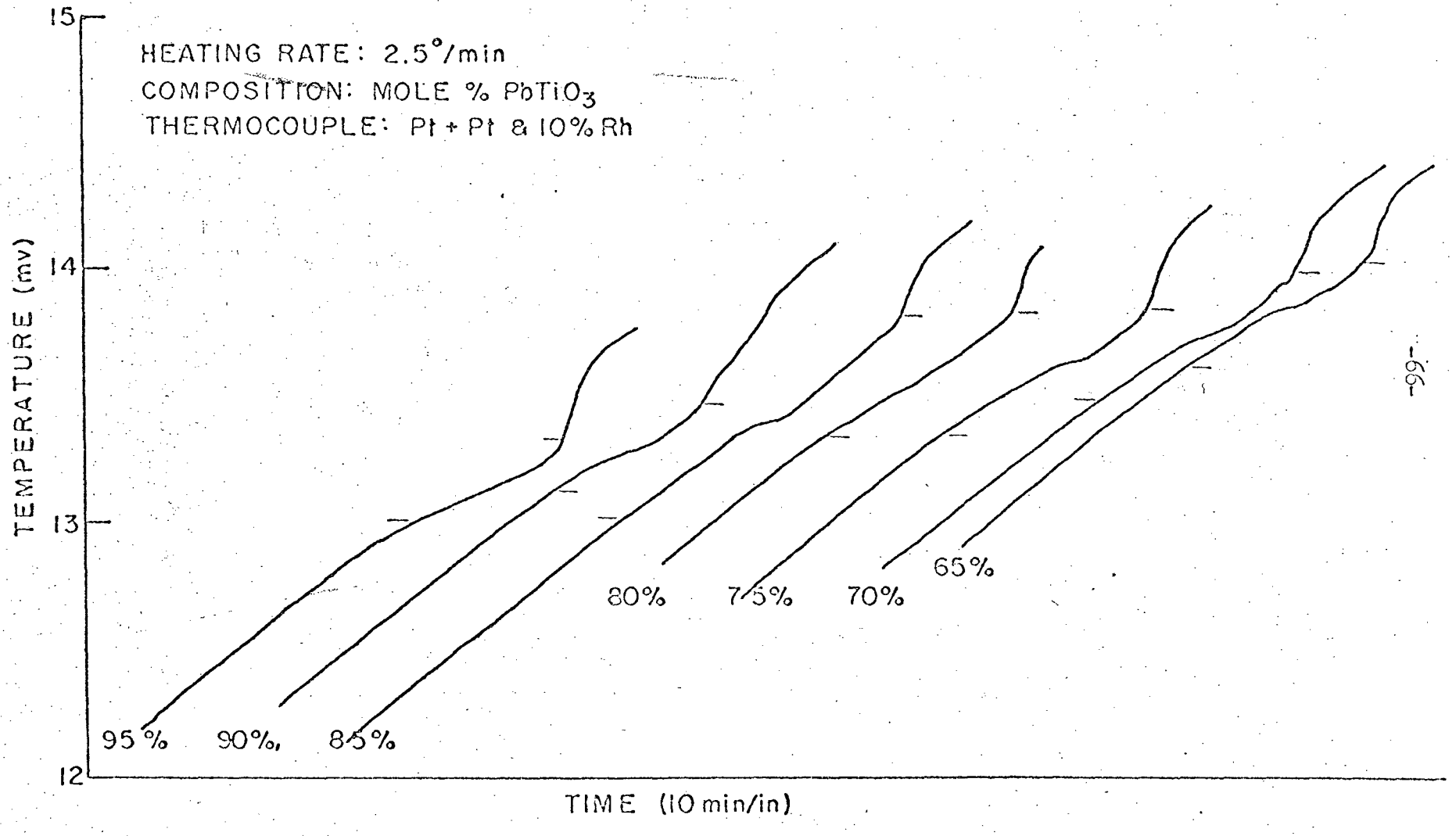

Fig. 25 Heating curves for a heating rate of 2.5°/min

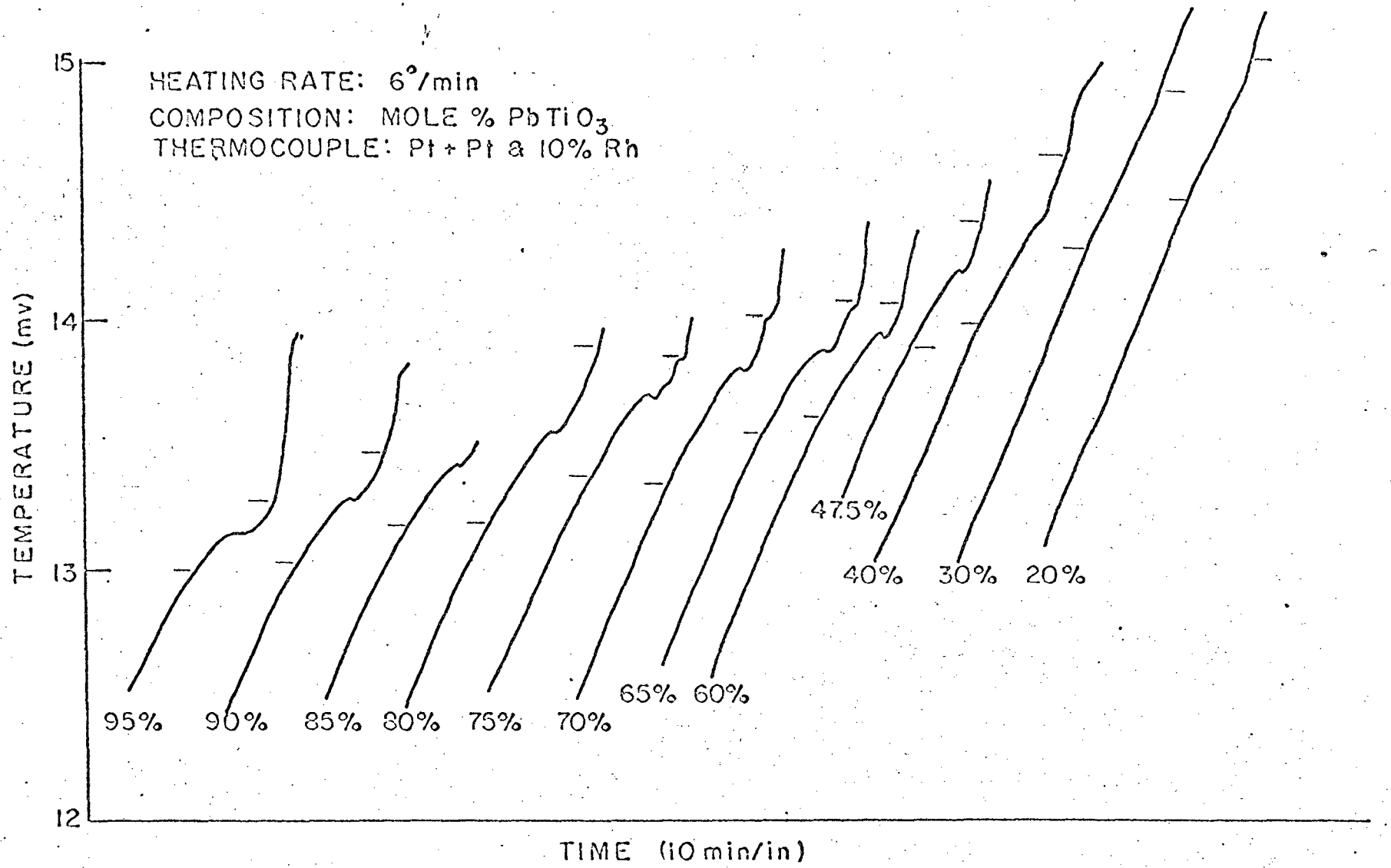

Fig. 26 Heating curves for a heating rate of 6°/min

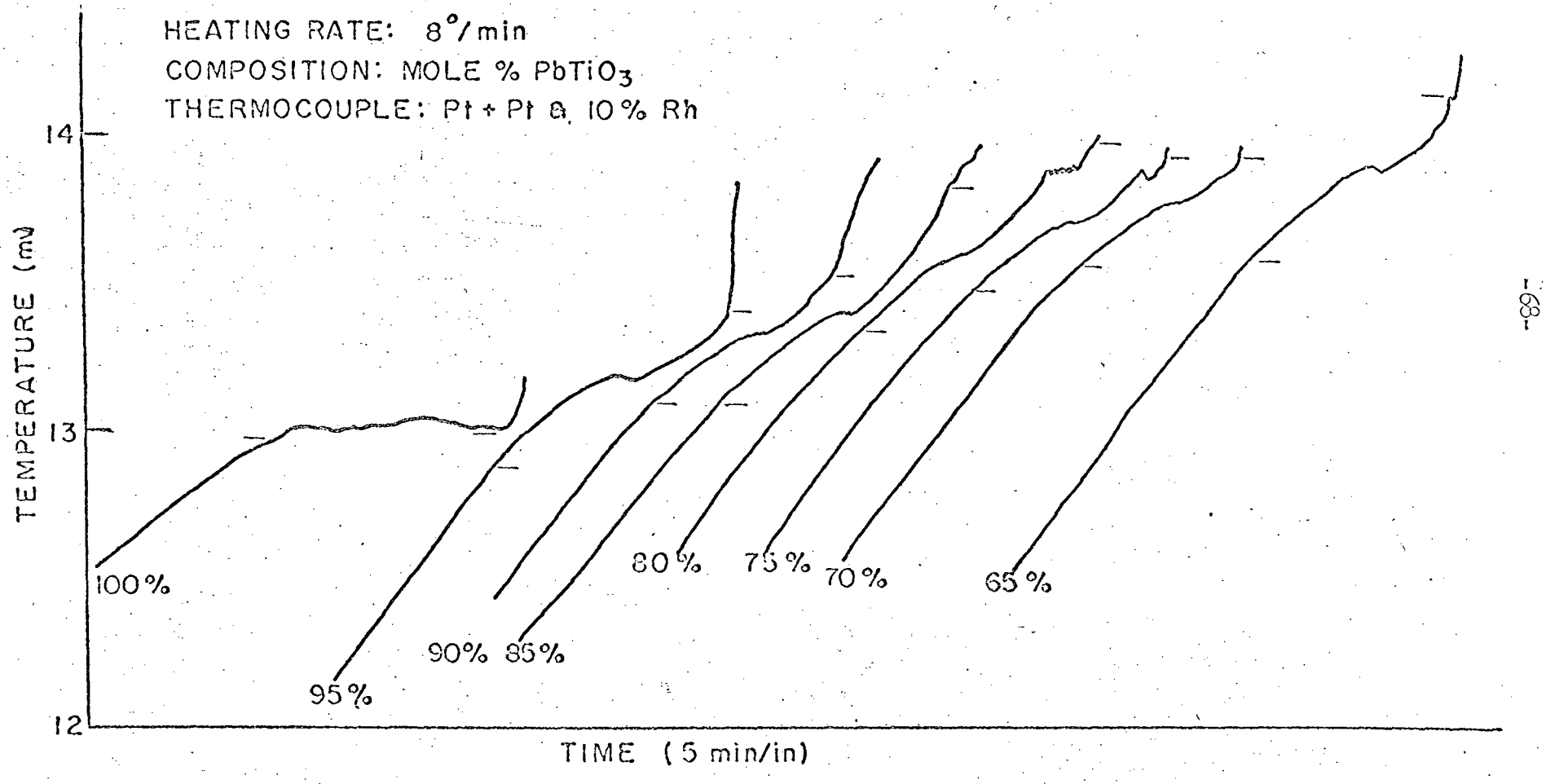

Fig. 27 Heating curves for a heating rate of 8°/min

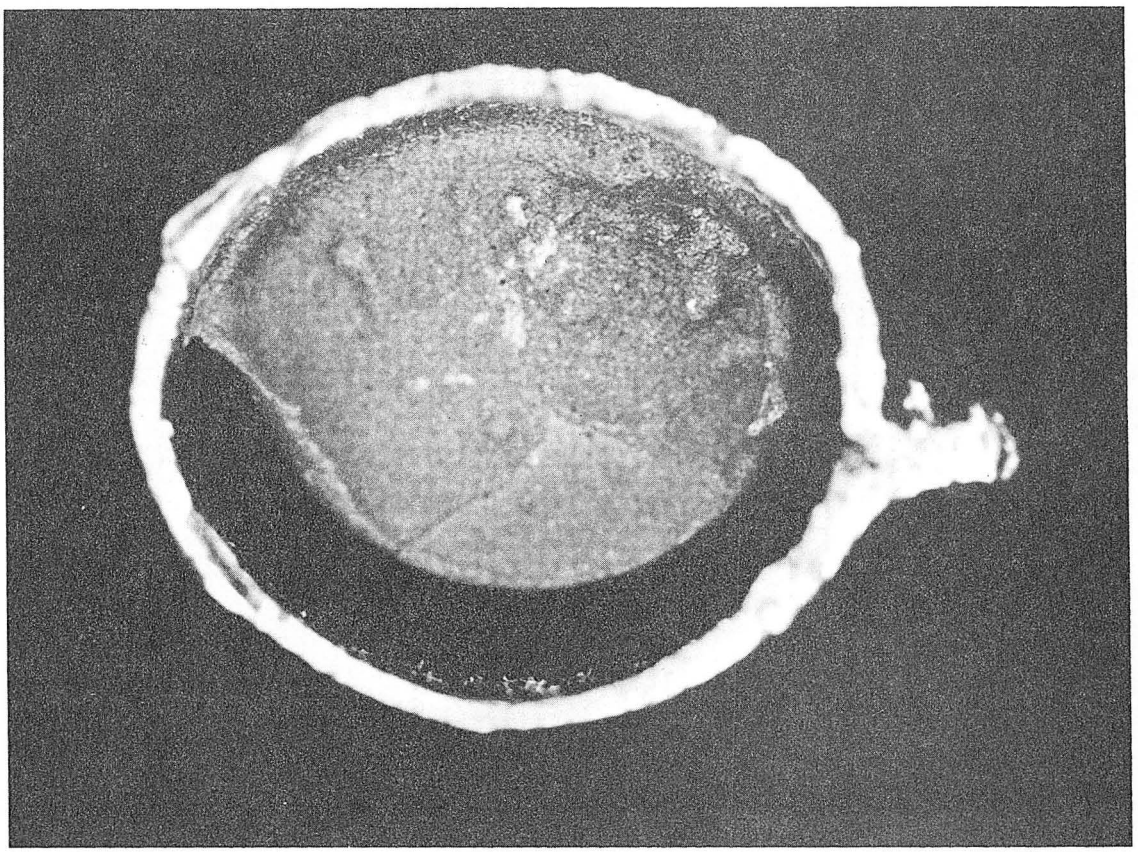

XBB 674-2063

Fig. 28. Cross-section of Pt crucible containing $Pb(Zr_{0.20}, Ti_{0.80}) O_3$ held at 1325°C.

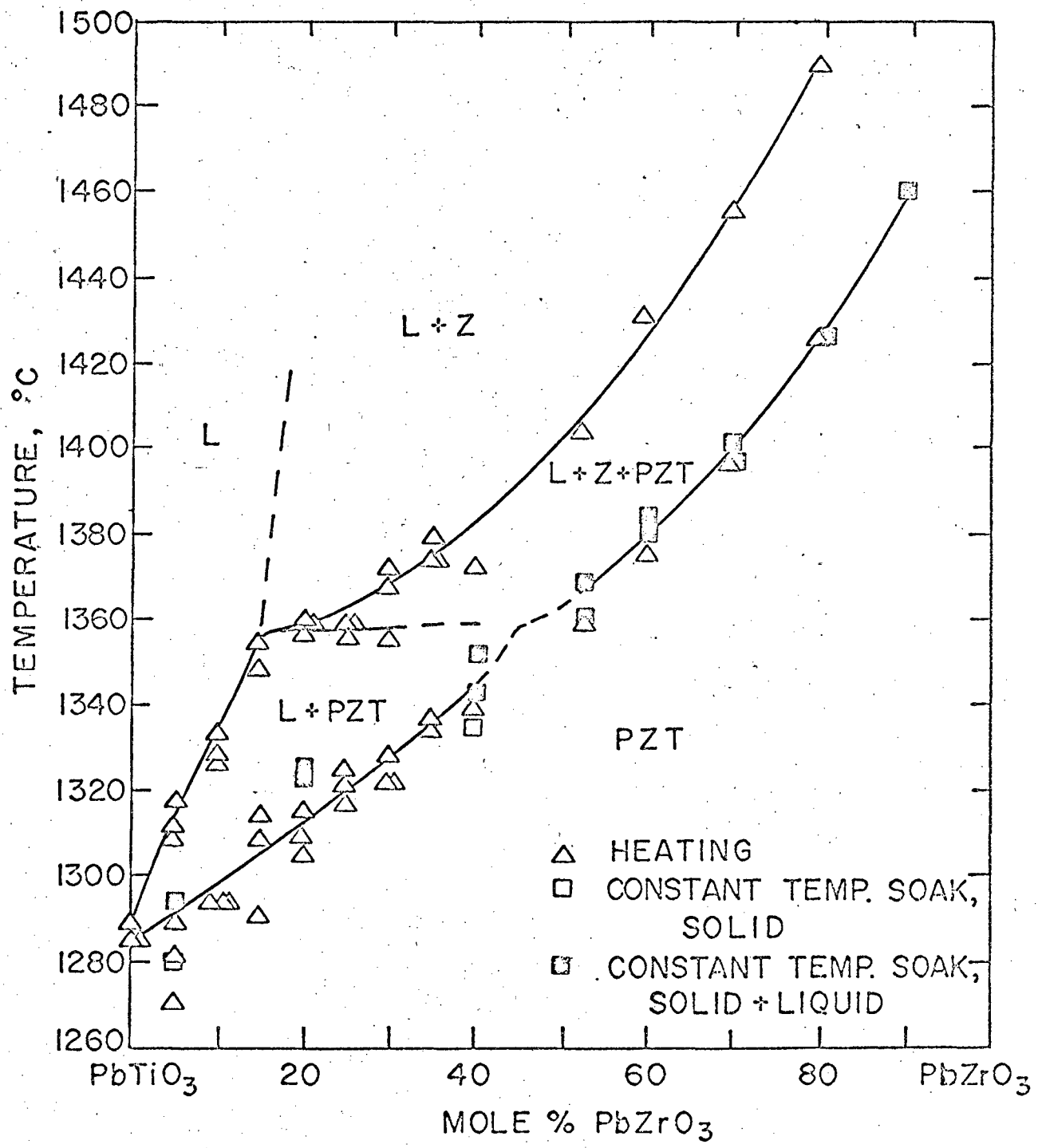

L = LIQUID

Z = ZrO_2 RICH SOLID

PZT = LEAD ZIRCONATE TITANATE

Fig. 29 Phase diagram determined by heating curve analysis

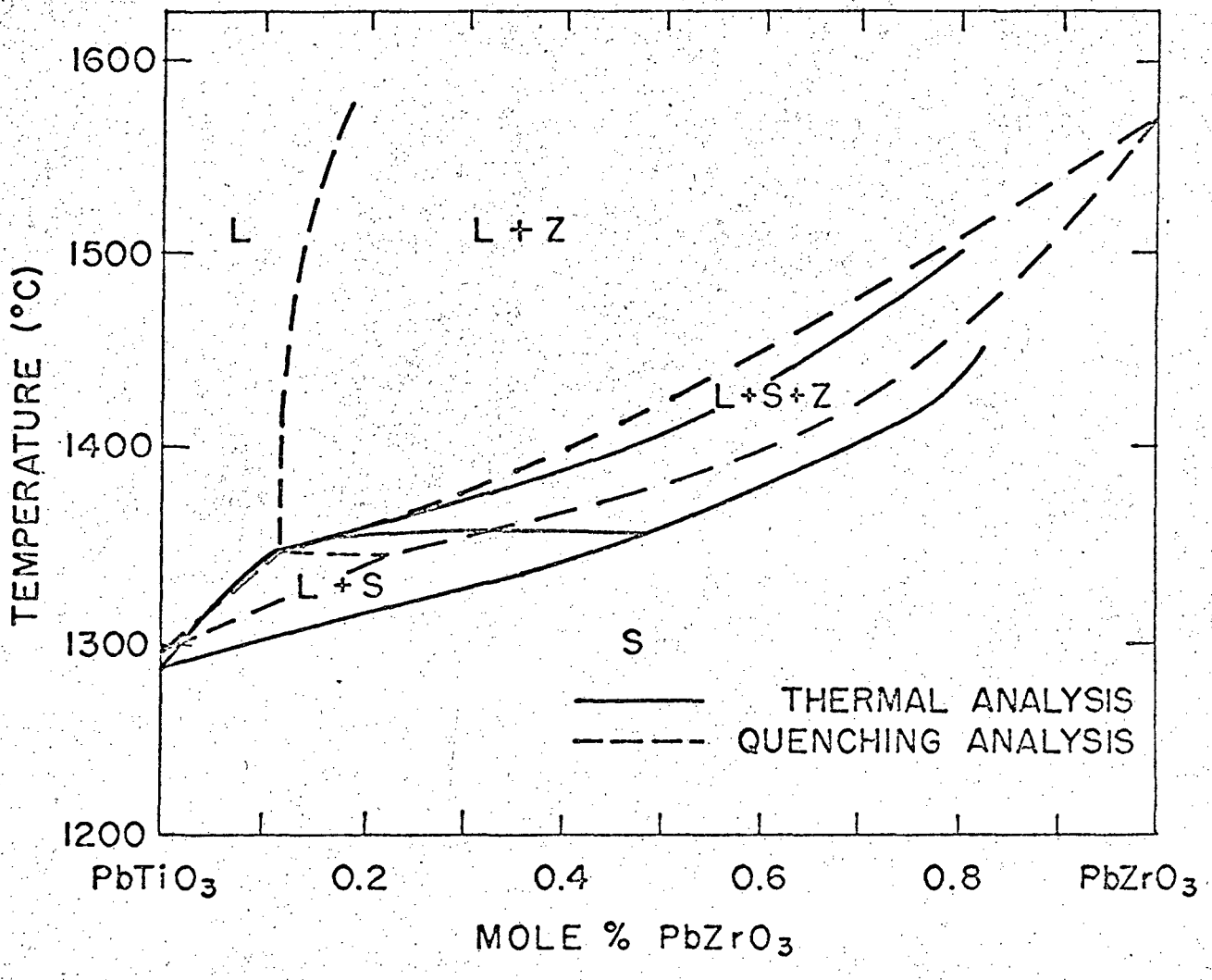

L = LIQUID
Z = ZrO_2 RICH SOLID
S = LEAD ZIRCONATE TITANATE

Fig. 30 Comparative phase diagrams based on thermal and quenching.[26]

APPENDIX I

Following is a table of interplanar spacings (d) in Å units vs the mole fraction (x) of $PbTiO_3$ in the lead titanate-lead zirconate system, $Pb(Ti_x, Zr_{1-x})O_3$, at room temperature. The indices of various planes are listed in the column at the left of the page.

Lattice constants were taken from data of B. Jaffe, S. R. Roth, and S. Marzullo, (N.B.S. 55, 239 (1955)). The lattice parameters were assumed to vary linearly with composition and were fitted to a straight line by a least means square procedure. Interplanar spacings were calculated from this data using the formulas for rhombohedral and tetragonal lattices (International Tables for X-ray Crystallography, Vol. I, N. F. M. Henry and K. Lonsdale, Editors, Kynoch Press, Birmingham, England, 1965)). All calculations were performed with a digital computer.

RHOMBOHEDRAL

P Q R	X= .10	.15	.20	.25	.30	.35	.40	.45
1 0 0	4.1384	4.1310	4.1235	4.1147	4.1058	4.0938	4.0817	4.0816
1 1 0	2.9336	2.9281	2.9225	2.9164	2.9102	2.9015	2.8927	2.8919
1 1 1	2.4013	2.3966	2.3918	2.3869	2.3820	2.3746	2.3672	2.3659
-1 1 1	2.3853	2.3812	2.3770	2.3719	2.3667	2.3599	2.3531	2.3534
2 0 0	2.0692	2.0655	2.0618	2.0573	2.0529	2.0469	2.0409	2.0408
-2 0 0	2.0692	2.0655	2.0618	2.0573	2.0529	2.0469	2.0409	2.0408
2 1 0	1.8544	1.8510	1.8475	1.8436	1.8397	1.8342	1.8287	1.8283
-2 1 0	1.8471	1.8439	1.8407	1.8367	1.8326	1.8274	1.8221	1.8225
2 1 1	1.6966	1.6933	1.6900	1.6865	1.6829	1.6778	1.6726	1.6718
2-1 1	1.6881	1.6851	1.6821	1.6785	1.6748	1.6700	1.6651	1.6652
-2 1 1	1.6853	1.6824	1.6795	1.6758	1.6722	1.6674	1.6626	1.6630
2 2 0	1.4668	1.4640	1.4613	1.4582	1.4551	1.4507	1.4463	1.4459
2 2 1	1.3856	1.3829	1.3802	1.3773	1.3745	1.3702	1.3660	1.3653
2 2-1	1.3795	1.3770	1.3745	1.3716	1.3686	1.3646	1.3606	1.3605
2 0 0	1.3795	1.3770	1.3745	1.3716	1.3686	1.3646	1.3606	1.3605
2-2 1	1.3764	1.3741	1.3717	1.3687	1.3657	1.3618	1.3579	1.3582
2 1 0	1.3106	1.3082	1.3058	1.3030	1.3002	1.2964	1.2925	1.2923
-2 1 0	1.3067	1.3044	1.3022	1.2993	1.2965	1.2928	1.2890	1.2892
3 1 1	1.2517	1.2494	1.2470	1.2444	1.2418	1.2380	1.2342	1.2338
-3 1-1	1.2472	1.2450	1.2428	1.2401	1.2374	1.2338	1.2302	1.2302
-3 1 1	1.2450	1.2428	1.2407	1.2380	1.2352	1.2317	1.2282	1.2285
2 2 2	1.2006	1.1983	1.1959	1.1935	1.1910	1.1873	1.1836	1.1829
-2 2 2	1.1927	1.1906	1.1885	1.1859	1.1833	1.1799	1.1765	1.1767
2 2 0	1.1504	1.1483	1.1461	1.1437	1.1413	1.1378	1.1344	1.1341
-2 2 0	1.1452	1.1432	1.1412	1.1387	1.1362	1.1330	1.1297	1.1300

RHOMBOHEDRAL

P Q R	X= .10	.15	.20	.25	.30	.35	.40	.45
3 2-1	1.1064	1.1044	1.1024	1.1001	1.0977	1.0945	1.0912	1.0912
-3 2 1	1.1033	1.1014	1.0995	1.0971	1.0947	1.0916	1.0885	1.0887
3-2 1	1.1041	1.1022	1.1002	1.0978	1.0954	1.0923	1.0891	1.0893
4 0 0	1.0346	1.0327	1.0309	1.0287	1.0265	1.0234	1.0204	1.0204
3 2 2	1.0064	1.0065	1.0045	1.0024	1.0003	.9972	.9941	.9936
4 1 0	1.0049	1.0030	1.0012	.9991	.9969	.9940	.9910	.9909
-4 1 0	1.0025	1.0008	.9990	.9968	.9947	.9918	.9889	.9890
3-2 2	1.0025	1.0008	.9990	.9968	.9947	.9918	.9889	.9890
-3 2 2	1.0014	.9996	.9979	.9957	.9936	.9907	.9879	.9881
4 1 1	.9779	.9760	.9742	.9721	.9701	.9672	.9642	.9640
3 3 0	.9779	.9760	.9742	.9721	.9701	.9672	.9642	.9640
4-1 1	.9752	.9734	.9717	.9696	.9675	.9647	.9618	.9618
-4 1 1	.9735	.9719	.9702	.9681	.9659	.9632	.9604	.9606
-3 3 0	.9730	.9713	.9697	.9676	.9654	.9627	.9599	.9602
3 3 1	.9532	.9513	.9495	.9475	.9455	.9426	.9397	.9393
4 2 0	.9272	.9255	.9238	.9218	.9199	.9171	.9143	.9141
-4 2 0	.9235	.9219	.9203	.9183	.9163	.9137	.9111	.9112
4 2 1	.9061	.9044	.9026	.9007	.8988	.8961	.8934	.8930
4 2-1	.9035	.9019	.9002	.8983	.8964	.8937	.8911	.8910
4-2 1	.9018	.9002	.8986	.8967	.8947	.8922	.8896	.8897
-4 2 1	.9009	.8994	.8978	.8959	.8939	.8914	.8888	.8890
3 3 2	.8865	.8848	.8831	.8812	.8794	.8767	.8740	.8735
-3 3 2	.8805	.8790	.8775	.8756	.8736	.8711	.8686	.8688
3 3-2	.8817	.8801	.8786	.8767	.8748	.8722	.8697	.8697
4 2 2	.8483	.8466	.8450	.8432	.8415	.8389	.8363	.8359

RHOMBOHEDRAL

P Q R	X=	.10	.15	.20	.25	.30	.35	.40	.45
-4 2 2		.8426	.8412	.8398	.8379	.8361	.8337	.8313	.8315
4 3 0		.8257	.8281	.8265	.8248	.8231	.8206	.8181	.8179
5 0 0		.8277	.8262	.8247	.8229	.8212	.8188	.8163	.8163
-4 3 0		.8257	.8243	.8229	.8211	.8193	.8169	.8146	.8148
5 1 0		.8124	.8109	.8094	.8077	.8060	.8036	.8012	.8011
4 3-1		.8124	.8109	.8094	.8077	.8060	.8036	.8012	.8011
-5 1 0		.8108	.8094	.8080	.8062	.8045	.8021	.7998	.7999
4-3 1		.8099	.8085	.8071	.8053	.8036	.8013	.7990	.7991
-4 3 1		.8096	.8082	.8068	.8051	.8033	.8010	.7987	.7989
3 3 3		.8004	.7989	.7973	.7956	.7940	.7915	.7891	.7886
5 1 1		.7981	.7966	.7951	.7934	.7917	.7893	.7870	.7868
5-1 1		.7963	.7949	.7934	.7917	.7900	.7877	.7854	.7854
-5 1 1		.7951	.7937	.7923	.7906	.7889	.7866	.7844	.7845
-3 3 3		.7951	.7937	.7923	.7906	.7889	.7866	.7844	.7845
-5 2 0		.7672	.7658	.7645	.7628	.7612	.7590	.7568	.7569
5 2 0		.7698	.7684	.7669	.7653	.7637	.7614	.7591	.7590

TETRAGONAL

P Q R	X=	.475	.50	.55	.60	.65	.70	.75	.80	.85	.90	.95	1.00
C 0 1		4.1383	4.1393	4.1407	4.1421	4.1431	4.1442	4.1457	4.1472	4.1487	4.1502	4.1517	4.1532
1 0 0		4.0448	4.0311	4.0178	4.0045	3.9925	3.9805	3.9671	3.9536	3.9402	3.9268	3.9133	3.8999
1 0 1		2.8926	2.8879	2.8835	2.8790	2.8749	2.8708	2.8662	2.8616	2.8570	2.8524	2.8477	2.8430
1 1 0		2.8601	2.8504	2.8410	2.8316	2.8231	2.8146	2.8051	2.7956	2.7861	2.7766	2.7671	2.7576
1 1 1		2.3529	2.3476	2.3426	2.3376	2.3330	2.3284	2.3233	2.3181	2.3130	2.3078	2.3026	2.2973
0 0 2		2.0691	2.0696	2.0703	2.0710	2.0716	2.0721	2.0728	2.0736	2.0743	2.0751	2.0758	2.0766
2 0 0		2.0224	2.0156	2.0089	2.0022	1.9962	1.9902	1.9835	1.9768	1.9701	1.9634	1.9567	1.9499
1 0 2		1.8421	1.8412	1.8404	1.8396	1.8388	1.8380	1.8372	1.8364	1.8355	1.8347	1.8338	1.8329
2 0 1		1.8170	1.8121	1.8074	1.8027	1.7984	1.7941	1.7893	1.7845	1.7796	1.7748	1.7699	1.7651
2 1 0		1.8089	1.8028	1.7968	1.7909	1.7855	1.7801	1.7741	1.7681	1.7621	1.7561	1.7501	1.7441
1 1 2		1.6764	1.6747	1.6732	1.6716	1.6702	1.6687	1.6671	1.6655	1.6638	1.6622	1.6605	1.6589
2 1 1		1.6575	1.6528	1.6483	1.6438	1.6397	1.6356	1.6310	1.6265	1.6219	1.6173	1.6127	1.6081
2 0 2		1.4463	1.4440	1.4417	1.4395	1.4375	1.4354	1.4331	1.4308	1.4285	1.4262	1.4238	1.4215
2 2 0		1.4301	1.4252	1.4205	1.4158	1.4116	1.4073	1.4026	1.3978	1.3931	1.3883	1.3836	1.3788
0 0 3		1.3794	1.3798	1.3802	1.3807	1.3810	1.3814	1.3819	1.3824	1.3829	1.3834	1.3839	1.3844
2 1 2		1.3619	1.3594	1.3570	1.3546	1.3525	1.3503	1.3479	1.3454	1.3430	1.3405	1.3380	1.3355
2 2 1		1.3516	1.3476	1.3436	1.3397	1.3361	1.3326	1.3286	1.3246	1.3206	1.3166	1.3126	1.3086
3 0 0		1.3483	1.3437	1.3393	1.3348	1.3308	1.3268	1.3224	1.3179	1.3134	1.3089	1.3044	1.3000
1 0 3		1.3056	1.3054	1.3054	1.3053	1.3052	1.3050	1.3050	1.3049	1.3049	1.3048	1.3047	1.3046
3 0 1		1.2819	1.2780	1.2743	1.2705	1.2671	1.2636	1.2598	1.2560	1.2522	1.2483	1.2445	1.2406
3 1 0		1.2791	1.2747	1.2705	1.2663	1.2625	1.2587	1.2545	1.2502	1.2460	1.2418	1.2375	1.2333
1 1 3		1.2425	1.2419	1.2415	1.2410	1.2406	1.2401	1.2396	1.2392	1.2387	1.2382	1.2377	1.2372
3 1 1		1.2220	1.2183	1.2146	1.2110	1.2077	1.2044	1.2007	1.1970	1.1933	1.1896	1.1859	1.1822
2 2 2		1.1764	1.1738	1.1713	1.1688	1.1665	1.1642	1.1616	1.1591	1.1565	1.1539	1.1513	1.1487
2 0 3		1.1396	1.1385	1.1376	1.1367	1.1357	1.1348	1.1339	1.1329	1.1319	1.1309	1.1299	1.1288

TETRAGONAL

P Q R	X= .475	.50	.55	.60	.65	.70	.75	.80	.85	.90	.95	1.00
2 2 0	1.1218	1.1180	1.1143	1.1106	1.1073	1.1040	1.1003	1.0965	1.0928	1.0891	1.0854	1.0816
2 1 3	1.0969	1.0957	1.0946	1.0935	1.0924	1.0913	1.0902	1.0890	1.0879	1.0867	1.0855	1.0843
3 1 2	1.0880	1.0854	1.0829	1.0804	1.0781	1.0758	1.0733	1.0707	1.0681	1.0655	1.0630	1.0604
3 2 1	1.0827	1.0793	1.0761	1.0728	1.0698	1.0668	1.0635	1.0601	1.0568	1.0534	1.0501	1.0467
0 0 4	1.0346	1.0348	1.0352	1.0355	1.0358	1.0360	1.0364	1.0368	1.0372	1.0375	1.0379	1.0383
1 0 4	1.0023	1.0023	1.0024	1.0025	1.0026	1.0026	1.0028	1.0029	1.0030	1.0031	1.0032	1.0033
4 0 0	1.0112	1.0078	1.0044	1.0011	.9981	.9951	.9918	.9884	.9850	.9817	.9783	.9750
2 2 3	.9928	.9913	.9899	.9885	.9872	.9858	.9844	.9829	.9814	.9799	.9784	.9769
3 2 2	.9862	.9837	.9812	.9788	.9766	.9743	.9718	.9694	.9668	.9643	.9618	.9593
4 0 1	.9823	.9792	.9761	.9731	.9704	.9676	.9646	.9615	.9584	.9553	.9523	.9492
4 1 0	.9810	.9777	.9745	.9712	.9683	.9654	.9622	.9589	.9556	.9524	.9491	.9459
1 1 4	.9729	.9727	.9726	.9725	.9724	.9723	.9722	.9721	.9720	.9719	.9718	.9717
4 1 1	.9546	.9515	.9485	.9456	.9429	.9402	.9372	.9342	.9313	.9283	.9253	.9222
2 0 3	.9642	.9626	.9612	.9597	.9583	.9569	.9554	.9539	.9523	.9508	.9492	.9477
3 3 0	.9534	.9501	.9470	.9439	.9410	.9382	.9350	.9319	.9287	.9255	.9224	.9192
2 0 4	.9211	.9206	.9202	.9198	.9194	.9190	.9186	.9182	.9178	.9173	.9169	.9165
2 1 3	.9379	.9363	.9348	.9333	.9318	.9304	.9288	.9273	.9257	.9241	.9225	.9209
3 3 1	.9290	.9261	.9232	.9203	.9177	.9151	.9121	.9092	.9063	.9034	.9004	.8975
2 1 4	.8981	.8975	.8970	.8965	.8959	.8954	.8949	.8944	.8938	.8933	.8927	.8922
4 0 2	.9065	.9061	.9037	.9013	.8992	.8970	.8946	.8922	.8898	.8874	.8850	.8825
4 2 0	.9044	.9014	.8984	.8954	.8928	.8901	.8871	.8841	.8811	.8781	.8750	.8720
4 1 2	.8864	.8840	.8817	.8793	.8772	.8751	.8727	.8703	.8680	.8656	.8632	.8608
4 2 1	.8836	.8807	.8780	.8752	.8727	.8702	.8674	.8646	.8618	.8590	.8562	.8534
2 2 3	.8703	.8686	.8670	.8654	.8639	.8624	.8608	.8591	.8574	.8557	.8540	.8523
3 3 2	.8659	.8635	.8612	.8589	.8568	.8547	.8523	.8500	.8476	.8453	.8429	.8405

TETRAGONAL

P Q R	X= .475	.50	.55	.60	.65	.70	.75	.80	.85	.90	.95	1.00
0 0 5	.8277	.8279	.8281	.8284	.8286	.8288	.8291	.8294	.8297	.8300	.8303	.8306
3 0 4	.8208	.8199	.8190	.8182	.8174	.8166	.8157	.8149	.8140	.8131	.8122	.8113
4 2 2	.8287	.8264	.8242	.8219	.8199	.8178	.8155	.8132	.8109	.8086	.8063	.8040
1 0 5	.8109	.8109	.8111	.8112	.8113	.8114	.8116	.8118	.8119	.8121	.8123	.8124
4 0 3	.8155	.8138	.8122	.8105	.8090	.8074	.8057	.8040	.8023	.8006	.7989	.7971
3 1 4	.8044	.8034	.8025	.8016	.8008	.7999	.7990	.7981	.7971	.7962	.7952	.7943
1 1 5	.7950	.7950	.7951	.7951	.7951	.7951	.7951	.7952	.7952	.7953	.7953	.7953
5 0 0	.8090	.8062	.8036	.8009	.7985	.7961	.7934	.7907	.7880	.7854	.7827	.7800
4 3 0	.8090	.8062	.8036	.8009	.7985	.7961	.7934	.7907	.7880	.7854	.7827	.7800
4 1 3	.7995	.7977	.7961	.7944	.7929	.7913	.7896	.7879	.7862	.7845	.7827	.7810
5 0 1	.7939	.7913	.7888	.7863	.7841	.7818	.7793	.7767	.7742	.7717	.7691	.7666
4 3 1	.7939	.7913	.7888	.7863	.7841	.7818	.7793	.7767	.7742	.7717	.7691	.7666
5 1 0	.7933	.7906	.7880	.7853	.7830	.7806	.7780	.7754	.7727	.7701	.7675	.7648
3 3 3	.7843	.7825	.7809	.7792	.7777	.7761	.7744	.7727	.7710	.7693	.7675	.7658
5 1 1	.7791	.7765	.7741	.7716	.7694	.7671	.7647	.7622	.7597	.7572	.7547	.7522
2 0 5	.7660	.7658	.7656	.7655	.7653	.7651	.7650	.7648	.7647	.7645	.7644	.7642
3 2 4	.7605	.7594	.7584	.7574	.7564	.7555	.7544	.7534	.7523	.7512	.7501	.7490
2 1 5	.7526	.7523	.7521	.7519	.7516	.7514	.7512	.7509	.7507	.7504	.7502	.7499
4 2 3	.7564	.7546	.7530	.7513	.7497	.7482	.7465	.7448	.7431	.7413	.7396	.7379
5 0 2	.7534	.7512	.7491	.7470	.7451	.7431	.7410	.7388	.7367	.7345	.7323	.7302
5 2 0	.7511	.7486	.7461	.7436	.7414	.7392	.7367	.7342	.7317	.7292	.7267	.7242
5 1 2	.7407	.7385	.7364	.7343	.7324	.7305	.7284	.7263	.7241	.7220	.7198	.7177
5 2 1	.7390	.7366	.7343	.7319	.7298	.7277	.7253	.7229	.7206	.7182	.7158	.7134
4 0 4	.7231	.7220	.7209	.7198	.7187	.7177	.7166	.7154	.7143	.7131	.7119	.7107
2 2 5	.7163	.7159	.7154	.7150	.7146	.7142	.7138	.7133	.7129	.7124	.7120	.7115

TETRAGONAL

P Q R	X= .475	.50	.55	.60	.65	.70	.75	.80	.85	.90	.95	1.00
3 0 5	.7054	.7048	.7044	.7039	.7034	.7030	.7025	.7020	.7015	.7010	.7005	.7000
5 2 2	.7060	.7039	.7019	.6999	.6980	.6962	.6941	.6921	.6900	.6879	.6859	.6838
3 3 4	.7011	.6999	.6987	.6976	.6965	.6954	.6943	.6931	.6919	.6907	.6895	.6883
5 0 3	.6978	.6961	.6944	.6928	.6913	.6898	.6881	.6864	.6847	.6830	.6813	.6795
4 3 3	.6978	.6961	.6944	.6928	.6913	.6898	.6881	.6864	.6847	.6830	.6813	.6795

APPENDIX II

The term "quasi binary" is occasionally misunderstood and thought to refer to a pseudo binary which is an equally confusing term. The definition given here is from Masing[53] (see pg. 45).

> "The solidification of all alloys on the section VC (a line connecting two compounds in a ternary system) follows exactly as for a binary alloy, and in no instance does the behavior of an alloy give any indication that it is a member of a ternary system. Such sections lying within a system of higher order but behaving like a binary alloy system are called 'quasi-binary sections'."

REFERENCES

1. G. Shirane, S. Hoskins, and K. Suzuki, X-ray Study of the Phase Transitions in Lead Titanate, Phys. Rev. 80, 1105 (1950).

2. G. A. Smolenskii, Doklady Akad. Nauk. SSSR 70, 405 (1950) not translated).

3. G. A. Smolenskii, Zhur. Teckh. Fiz. 20, 137 (1950) (not translated).

4. J. Kobayashi and R. Ueda, X-ray Study of Phase Transitions of Ferroelectric $PbTiO_3$ at Low Temperatures, Phys. Rev. 99, 1900 (1955).

5. G. Shirane and S. Hoshino, On the Phase Transitions in Lead Titanate, J. Phys. Soc. Japan, 6, 265 (1951).

6. H. Swanson, N. Gilfrich, and G. Ugrinic, Lead Titanate (Tetragonal), NBS Circular 539, Vol. V (1955).

7. G. Shirane, K. Suzuki and A. Takeda, Phase Transitions in Solid Solutions of $PbZrO_3$ and $PbTiO_3$ (II), J. Phys. Soc. Japan 7, [1] 12-18 (1952).

8. G. Shirane, R. Pepinsky, and B. C. Frazer, X-ray and Neutron Diffraction Study of Ferroelectric $PbTiO_3$, Acta Cryst. 9, 131 (1956).

9. H. Rogers, The Growing of $PbTiO_3$ Crystals and Some of Their Properties, Lab for Insulation Research, M.I.T., ONR Contracts N5ori07801, N5ori07858, Dec. 1952.

10. J. Kobayashi, Growing of Ferroelectric $PbTiO_3$ Crystals, J. Appl. Phys. 29, 866 (1958).

11. E. G. Fesenko, O. P. Kramaror, A. L. Kodakov, and M. L. Sholokhovich, Growing and Investigation of Ferroelectric Single Crystals, Izvest. Akad. Nauk. SSSR Ser Fiz 21, 305 (1957).

12. M. L. Sholokovick, E. G. Fesnko, O. P. Kararov, and A. L. Rhodakov, Dolady Akad. Nauk SSSR iii, 1025 (1956) (not translated).

13. S. Normura and S. Savada, Rept. Inst. Sci. Technol., Univ. Tokyo 6 191 (1952).

14. Kyoski Okazaki, High Permittivity Ceramics Containing Lead Monoxide and its Evaporations at High Temperature, Yogyo Kyokai Shi 66, (755) 260-66 (1958).

15. R. S. Roth, private communication to Shoichi Fushimi and Takuso Ikeda, PhaseEquilibrium in the System PbO-TiO_2-ZrO_2, J. Am. Ceram. Soc. 50, 3, 129-132 (1967).

16. T. Ikeda, T. Oakno, M. Watanabe, A Ternary System PbO-TiO_2-ZrO_2. Japan J. Appl. Phys. 1, 4, 218 (1962).

17. I. N. Belyaer and A. K. Nesterva, The Fusibility of the Ternary System: PbO-V_2O_5, J. Gen. Chem. USSR 22, 402 (1952).

18. Yoshihiro Matsuo and Heromu Sasaki, PbO Rich Side of the System PbO-TiO_2, J. Am. Ceram. Soc. 46, 8, 409 (1963).

19. S. Roberts, Dielectric Properties of Lead Zirconate and Barium-Lead Titanate, J. Am. Ceram. Soc. 33, 63 (1950).

20. L. Goulpeau, Two Phase Transitions in Lead Zirconate, Soviet Phys.-Solid State 8, 8, 1970 (1967).

21. J. Tennery, A Study of the Phase Transitions in $PbZrO_3$, J. Electrochem. Soc. 112, 11, (1965).

22. E. Sawaguchi, G. Shirane, Y. Takagi, Phase Transitions in Lead Zirconate, J. Phys. Soc. Japan 6, 33 (1951).

23. E. Sawaguchi, H. Manwa, and S. Hoshino, Antiferroelectric Structure of Lead Zirconate, Phys. Rev. 83, 1078 (1951).

24. H. D. McGaw, Crystal Structure of Double Oxides of the Perovskite Type, Proc. Phys. Soc. (London) 58, Part 2, 326, p. 133 (1946).

25. F. Jona, G. Shirane, F. Mazzi, R. Pepinsky, X-ray and Neutron Diffraction Study of Pb-ZrO_3, Phys. Rev. 105, 849 (1957).

26. Shoichi Fushimi and Takuro Ikeda, Phase Equilibrium in the System PbO-TiO_2-ZrO_2, J. Am. Ceram. 50, 3, 129-132 (1967).

27. H. J. Stocker, Contribution a L'Etude des Proprietes des Solutions Solides Refractaires a Base de Zircone et de la Stabilisation de la Zircone Cubique, Ann. Chim. 5, 11-12, 1459 (1960).

28. A. F. Robinson and T. A. Joyce, Preparation of Lead Zirconate-Titanate Compositions. I Determination of Unreacted Constituents, Trans. Brit. Ceram. Soc. 61 (2), 85-93 (1962).

29. F. Jona, G. Shirane, and P. Pepinsky, Optical Studies of $PbZrO_3$ and $NaNbO_3$ Single Crystals, Phys. Rev. 97, 1584 (1955).

30. F. Jona and G. Shirane, Ferroelectric Crystals, (Macmillan Pub. Co., New York, 1962).

31. Saburo Mori, Hironuchi Mitsuda, Kenju Date, Yashuhiro Hioki, and Toshihiko Mizazawa, Study of Formation Process of $Pb(Ti,Zr)O_3$ Solid Solution with High Temperature X-ray Diffractometry and Differential Thermal Analysis, Matsushita Electrical Ind., Co., Nat. Tech. Report 10, 1, p. 32-40 (1964).

32. G. Shirane and A. Takeda, Phase Transitions in Solid Solutions of $PbZrO_3$ and $PbTiO_3$ (I) Small Concentrations of $PbTiO_3$, J. Phys. Soc. Japan 7, 1, 5 (1952).

33. E. Sawaguchi, Ferroelectricity vs Antiferroelectricity in Solid Solution of $PbZrO_3$ and $PbTiO_3$, J. Phys. Soc. Japan 8, 615 (1953).

34. B. Jaffe, R. S. Roth, and S. Marzullo, Piezoelectric Properties of PZT Solid Solution Ceramics, J. Appl. Phys. 25, 809-810 (1954).

35. B. Jaffe, R. S. Roth, and S. Marzullo, Properties of Piezoelectric Ceramics in the Solid Series Lead Titanate-Lead Zirconate-Lead Oxide: Tin Oxide and Lead Titanate-Lead Hafnate, N.B.S. 55, 239 (1955).

36. A. H. Webster, R. C. MacDonald and W. S. Bowman, The System $PbO-ZrO_2-TiO_2$ at 1100°C, J. Can. Ceram. Soc. 34, 97-102 (1965).

37. Kaneomi Nagase and Tsuneharu Nitta, Evaporation from $Pb(Ti_{1-x}Zr_x)O_3$ Compositions on Firing, Matsushita Elec. Ind. Co. National Tech. Rept. 10, 2, 162-169 (1964).

38. T. Ikeda and S. Fashimi, Preliminary Study on the Growth of Lead Zirconate-Titanate Crystals, J. Phys. Soc. Japan 17, 1202-1203 (1962).

39. S. Fushimi and T. Ikeda, Single Crystals of Lead Zirconate-Titanate Solid Solution, Japan J. Appl. Phys. 3, 171-172 (1964).

40. V. M. McNamara, A Wet Chemical Method for the Preparation of Oxide Mixtures Applicable to Electronic Ceramics, J. Can. Ceram. Soc. 34 103-120 (1965).

41. A. H. Webster, T. B. Weston, R. R. Craig, Some Ceramic and Electrical Properties of Bodies Fabricated from Co-precipated Lead Zirconium-Titanate Hydroxides, J. Can. Ceram. Soc. 34, 121-129 (1965).

42. D. J. Barkley, A. Hitchen, G. Zechanowitsch, J. B. Zimmerman, and J. C. Ingles, J. Can. Ceram. Soc. 34, p. 130-136 (1965).

43. K. S. Valeer and I. A. Gai, Process of Formation of Titanates and Zirconates, Trudy Cosudurst Issledovatal Electrokeram Inst. 2, 39-53 (1957); Chem. Abst. Nov. 1960, 25661 g.

44. Y. Matsuo and H. Sasaki, Formation Process of Lead Zirconate-Lead Titanate in the System $PbO-TiO_2-ZrO_2$, J. Am. Ceram. Soc. 48, 6, p. 289-291 (1965).

45. N. H. Furman, Editor, Scott's Standard Methods of Chemical Analysis, 6th Edition, Vol. 1 (Van Nostrand Co., Inc., New York, 1962).

46. I. M. Kolthoff and P. J. Elving, Treatise of Analytical Chemistry, (Interscience Pub., New York, 1961).

(a) Part II, Vol. 5

(b) Part II, Vol. 6

47. Charles D. Hodgman, Editor, Handbook of Physics and Chemistry, (Chemical Rubber Publ. Co., Cleveland, Ohio, 1958).

48. E. G. King, D. R. Torgeson and O. A. Cook, High Temperature Heat Contents of $3CaO-B_2O_3$, $2CaO-B_2O_3$ and $CaO-2B_2O_3$, J. Am. Chem. Soc. 70, 2170 (1948).

49. J. A. Pask and M. F. Warner, Differential and Thermal Analysis Methods and Techniques, Am. Ceram. Soc. Bull. 33, 6 (1954).

50. H. Thomann, Relation of Lead Vaporization and the Concentration of Lead Deficiencies in Lead Zirconate-Titanate Ceramics, Keram Z. 18, [9], 645-46 (1966); J. Am. Ceram. Soc. Abstr. 50, 3, 16, Mar. 1967.

51. W. P. White, Melting Point Determination, Am. J. Sci. 178, 453 (1909).

52. F. N. Rhines, Phase Diagrams in Metallurgy (McGraw-Hill Book Co., New York, 1956).

53. G. Masing, Ternary Systems, (translated by B. A. Rogers), (Dover Publications Inc., New York, 1960).